

# IMPLEMENTATION OF EQUIVALENT DOMAIN INTEGRAL METHOD IN THE TWO-DIMENSIONAL ANALYSIS OF MIXED MODE PROBLEMS

I. S. Raju and K. N. Shivakumar  
Analytical Services and Materials, Inc.,  
107 Research Drive, Hampton Va. 23666

## Abstract

An equivalent domain integral (EDI) method for calculating  $J$ -integrals for two-dimensional cracked elastic bodies is presented. The details of the method and its implementation are presented for isoparametric elements. The total and product integrals consist of the sum of an area or domain integral and line integrals on the crack faces. The line integrals vanish only when the crack faces are traction free and the loading is either pure mode  $I$  or pure mode  $II$  or a combination of both with only the square-root singular term in the stress field. The EDI method gave accurate values of the  $J$ -integrals for two mode  $I$  and two mixed mode problems. Numerical studies showed that domains consisting of one layer of elements are sufficient to obtain accurate  $J$ -integral values. Two procedures for separating the individual modes from the domain integrals are presented. The procedure that uses the symmetric and antisymmetric components of the stress and displacement fields to calculate the individual modes gave accurate values of the integrals for all problems analyzed. The EDI method when applied to a problem of an interface crack in two different materials showed that the mode  $I$  and mode  $II$  components are domain dependent while the total integral is not. This behavior is caused by the presence of the oscillatory part of the singularity in bimaterial crack problems. The EDI method, thus, shows behavior similar to the virtual crack closure method for bimaterial problems.

## INTRODUCTION

Stress-intensity factors or strain-energy release rates are used to characterize the severity of the stress and strain fields at cracks or delaminations in elastic bodies. Numerous procedures exist in the literature to compute the stress-intensity factors or strain-energy release rates by analytical and numerical methods. For cracks in elastic-plastic materials, the  $J$ -integral was proposed [1-3]. As originally formulated, the  $J$ -integral is a closed contour integral of the strain-energy density and work done by tractions around the crack tip. The  $J$ -integral is a path-independent parameter and is equivalent to the rate of change of total potential energy with reference to the crack length. For elastic bodies the  $J$ -integral is equivalent to the strain-energy release rate.

Although the  $J$ -integral is a potential parameter to define the severity of the crack tip in elastic and elastic-plastic materials, it is cumbersome to compute in finite element analyses. Therefore, alternate forms of computing this integral have been proposed [4-11]. In references 6 and 7, procedures based on the virtual crack extension technique [4,5] were proposed to compute the strain-energy release rates (and hence the  $J$ -integral). In references 8 through 10 line  $J$ -integrals were converted to equivalent area or domain integrals, hence the name equivalent domain integral (EDI). The conversion of line integrals to domain integrals is very attractive because all the quantities necessary for computation of the domain integrals are readily available in a finite element analysis.

The potential of the EDI method appears to be in the calculation of the  $J$ -integrals (and the strain-energy release rates,  $G$ , for elastic materials) for three-dimensional (3D) crack configurations. With this method the  $J$ - or  $G$ -values can be computed at any point on the crack front in a straightforward manner. The force method [12] and virtual crack closure method [13], used for 3D crack configurations, require that the finite element mesh be normal to the crack front. In contrast, the EDI method does not require such customized modeling. The EDI method also appears to be a powerful tool to calculate the  $J$ -integrals for elastic-plastic materials and problems involving other material nonlinearities. Although the long term objectives of the present research are to apply the EDI method to 3D elastic and elastic-plastic problems, issues such as the mode separation in mixed mode situations and problems where the crack faces are subjected to external loading need to be addressed. These issues are studied for elastic two-dimensional crack configurations. Therefore, the purpose of this report is to address these two specific issues. First, a detailed formulation of the EDI method applicable to mixed mode problems under general loading is presented. Second methods for the separation of modes in mixed mode crack problems are studied.

As this report is intended to explore the method, the EDI method and its numerical implementation in the context of a finite element analysis with isoparametric elements is also presented. The method is then applied to two mode *I* problems and two mixed mode problems to study the sensitivity of fracture parameters to variables used in the EDI algorithm and to evaluate the methods for the separation of modes in mixed mode problems.

## SYMBOLS

- $a$  half-length or length of crack
- $b$  half-width or width of plate
- $D_i$   $i^{th}$  domain considered in the domain integral evaluation
- $E$  Young's modulus of the homogeneous material
- $E_1, E_2$  Young's moduli of materials 1 and 2 in a bimaterial plate
- $J_I, J_{II}$  mode *I* and mode *II* *J*-integrals
- $J_{ASx_1}, J_{ASx_2}$  Antisymmetric *J* and product integrals
- $J_{Sx_1}, J_{Sx_2}$  Symmetric *J* and product integrals
- $J_{x_1}, J_{x_2}$  *J* and product integrals
- $[J]$  Jacobian matrix of an isoparametric element
- $N_j$  shape function for the  $j^{th}$  node of an isoparametric element
- $n$  normal vector to the contour  $\Gamma$
- $n_j$  component of the normal  $n$  in the  $j^{th}$  direction
- $p$  remote uniform applied stress or uniform crack face pressure loading
- $S$  S-function defined in Eq. (7)
- $u_1, u_2$  displacements in the  $x_1$ - and  $x_2$ -directions, respectively
- $u_{1AS}, u_{2AS}$  antisymmetric components of displacements in the  $x_1$ - and  $x_2$ -directions, respectively

$u_{1S}, u_{2S}$  symmetric components of displacements in the  $x_1$ - and  $x_2$ -directions, respectively

$W$  strain-energy density

$x_1, x_2$  Cartesian coordinates

$\Gamma, \Gamma_0, \Gamma_1$  contours around the crack tip

$\epsilon_{ij}$  strain tensor

$\nu$  Poisson's ratio of a homogeneous material

$\nu_1, \nu_2$  Poisson's ratios of materials 1 and 2 of a bimaterial plate

$\sigma_{ij}$  stress tensor

Superscripts:

T denotes the transpose of a matrix or column vector

## CONTOUR AND DOMAIN INTEGRALS

Consider a crack in a plate subjected to an arbitrary remote loading with an arbitrary closed contour  $\Gamma$  around the crack tip, as shown in Figure 1. Then the  $J$ -integral is defined in the absence of any body forces as [1-3]

$$J_{x_k} = \int_{\Gamma} Q \, d\Gamma \quad (1)$$

where  $k = 1, 2$  and

$$Q = [W n_k - \sigma_{ij} \frac{\partial u_i}{\partial x_k} n_j] \quad (2)$$

In Eq. (2)  $W$  is the total strain-energy density defined as

$$W = \int_0^{\epsilon_{ij}} \sigma_{ij} d\epsilon_{ij} \quad (3)$$

In Eqs. (2) and (3)  $\sigma_{ij}$  is the stress tensor,  $\epsilon_{ij}$  is the total strain (which is the sum of the elastic and plastic strains) and  $n_j$  is the component in the  $j^{th}$  direction of the vector  $\mathbf{n}$  normal to the contour  $\Gamma$ . The indices  $i, j$ , and  $k$  take the values 1 and 2 for two-dimensional (2D) problems. The  $x_1$  and  $x_2$  represent the directions along and normal to the crack line, respectively.

The integrals  $J_{x_1}$  and  $J_{x_2}$  are two path-independent integrals that define the total amount of the energy flux leaving the contour  $\Gamma$  in the two directions  $x_1$  and  $x_2$ , respectively.  $J_{x_1}$  is usually termed the  $J$ -integral and  $J_{x_2}$  is called the product integral.

As previously mentioned, the line integrals of Eq. (1) are cumbersome to compute in a finite element analysis. In contrast, an area or domain integral is very convenient to compute in a finite element analysis. Therefore, an alternate form of Eq. (1), called the equivalent domain integral (EDI), was proposed [8,10,11]. A more detailed formulation of the EDI applicable for mixed mode problems and its numerical implementation is presented here.

Consider two contours  $\Gamma_0(OABCO)$  and  $\Gamma_1(ODEFO)$  around the crack tip as shown in Figure 1(b). The two contours will enclose an area  $DEFCBAD$ . By multiplying the integral over  $\Gamma_0$  by unity and the integral over  $\Gamma_1$  by zero,  $J_{x_k}$  can be expressed as

$$J_{x_k} = 1 \int_{\Gamma_0} Q d\Gamma - 0 \int_{\Gamma_1} Q d\Gamma \quad (4)$$

This manipulation is performed to convert the line integrals into an area or a domain integral. Equation (4) can be expanded as

$$\begin{aligned} J_{x_k} = & 1 \int_{ABC} Q d\Gamma - 0 \int_{DEF} Q d\Gamma \\ & + 1 \int_{CO} Q d\Gamma + 1 \int_{OA} Q d\Gamma \end{aligned} \quad (5)$$

An arbitrary but continuous function  $S(x_1, x_2)$  is introduced that has the property

$$S(x_1, x_2) = 1$$

on  $\Gamma_{ABC}$  and

$$S(x_1, x_2) = 0 \quad (6)$$

on  $\Gamma_{DEF}$ . Using this S-function, Eq. (5) can be written as

$$\begin{aligned} J_{x_k} &= \int_{ABC} Q S d\Gamma - \int_{DEF} Q S d\Gamma + \int_{CO} Q d\Gamma + \int_{OA} Q d\Gamma \\ &= \left[ - \int_{CBA} Q S d\Gamma - \int_{DEF} Q S d\Gamma \right] + \int_{CO} Q d\Gamma + \int_{OA} Q d\Gamma \end{aligned} \quad (7)$$

A closed contour integral along  $DEFCBAD$  can be defined easily by adding and subtracting the line integrals on the crack faces  $FC$  and  $AD$  as

$$\begin{aligned} J_{x_k} &= - \int_{CBA} Q S d\Gamma - \int_{DEF} Q S d\Gamma - \int_{FC} Q S d\Gamma \\ &\quad + \int_{FC} Q S d\Gamma - \int_{AD} Q S d\Gamma + \int_{AD} Q S d\Gamma \\ &\quad + \int_{CO} Q d\Gamma + \int_{OA} Q d\Gamma \\ &= - \int_{DEFCBAD} Q S d\Gamma + \int_{FC} Q S d\Gamma + \int_{AD} Q S d\Gamma \\ &\quad + \int_{CO} Q d\Gamma + \int_{OA} Q d\Gamma \end{aligned} \quad (8)$$

or

$$J_{x_k} = - \int_{DEFCBAD} Q S d\Gamma + (J_{x_k})_{line} \quad (9)$$

In Eq. (9), the first term on the right hand side is an integral on the closed contour  $DEFCBAD$  that excludes the crack tip. The second term on the right

hand side of the Eq. (9) corresponds to the line integrals on the crack faces. As will be shown below, the closed contour integral can be converted to an area or a domain integral. Hence,  $J_{x_k}$  can be written as

$$J_{x_k} = (J_{x_k})_{domain} + (J_{x_k})_{line} \quad (10)$$

Closed Contour Integral – Invoking the divergence theorem, the closed contour integral of Eq. (9) can be converted to a domain integral as

$$\begin{aligned} - \int_{DEFCBAD} Q S d\Gamma &= - \int_{DEFCBA} [W n_k - \sigma_{ij} \frac{\partial u_i}{\partial x_k} n_j] S d\Gamma \\ &= - \int_A \left[ \frac{\partial(WS)}{\partial x_k} - \frac{\partial(\sigma_{ij} \frac{\partial u_i}{\partial x_k} S)}{\partial x_j} \right] dA \end{aligned} \quad (11)$$

Hence, the domain integral is

$$\begin{aligned} (J_{x_k})_{domain} &= - \int_A \left[ W \frac{\partial S}{\partial x_k} - \sigma_{ij} \frac{\partial u_i}{\partial x_k} \frac{\partial S}{\partial x_j} \right] dA \\ &\quad - \int_A \left[ \frac{\partial W}{\partial x_k} - \sigma_{ij} \frac{\partial \epsilon_{ij}}{\partial x_k} \right] S dA \end{aligned} \quad (12)$$

In deriving Eq. (12) the equations of equilibrium

$$\frac{\partial \sigma_{ij}}{\partial x_j} = 0$$

and the strain-displacement relationships

$$\epsilon_{ij} = \frac{1}{2} \left( \frac{\partial u_i}{\partial x_j} + \frac{\partial u_j}{\partial x_i} \right)$$

were used.

In conventional finite element analysis, the equations of equilibrium are not satisfied pointwise in the domain that is modeled. Numerical experimentation showed that the differences between including and not including the terms involving the equations of equilibrium are of the order of  $10^{-3}$  to  $10^{-4}$  of the integral values for several problems. Therefore, in writing Eq. (12) the equations of equilibrium are assumed to be satisfied exactly.

The term in brackets in the second integral in Eq. (12) is identically equal to zero pointwise for a linear elastic material. This term, however, is non zero in elastic-plastic problems. Although only linear elastic materials are considered in this report, this term is included because the algorithm is intended for use with nonlinear material problems.

The domain integral in Eq. (12) can be rewritten in a form convenient to numerical computation as

$$\begin{aligned} (J_{x_k})_{domain} = & - \int_A \left[ W \frac{\partial S}{\partial x_k} - \{u'_{x_k}\}^T [\underline{\sigma}] \{S'\} \right] dA \\ & - \int_A \left[ \frac{\partial W}{\partial x_k} - \{\sigma\}^T \{\epsilon'_{x_k}\} \right] S dA \end{aligned} \quad (13)$$

where

$$\begin{aligned} \{\sigma\}^T &= \{ \sigma_{11} \quad \sigma_{12} \quad \sigma_{22} \} \\ \{\epsilon'_{x_k}\}^T &= \left\{ \frac{\partial \epsilon_{11}}{\partial x_k} \quad 2 \frac{\partial \epsilon_{12}}{\partial x_k} \quad \frac{\partial \epsilon_{22}}{\partial x_k} \right\} \\ \{u'_{x_k}\}^T &= \left\{ \frac{\partial u_1}{\partial x_k} \quad \frac{\partial u_2}{\partial x_k} \right\} \\ [\underline{\sigma}] &= \begin{bmatrix} \sigma_{11} & \sigma_{12} \\ \sigma_{12} & \sigma_{22} \end{bmatrix} \\ \{S'\}^T &= \left\{ \frac{\partial S}{\partial x_1} \quad \frac{\partial S}{\partial x_2} \right\} \end{aligned} \quad (14)$$

The strain-energy density  $W$  is

$$W = \frac{1}{2} [\sigma_{11}\epsilon_{11} + \sigma_{22}\epsilon_{22} + 2\sigma_{12}\epsilon_{12}] \quad (15)$$

The numerical implementation of Eq. (13) in a finite-element analysis with isoparametric elements is presented in Appendix A.

The integral  $J_{x_1}$  in Eq. (13) for the linear elastic case is equivalent to the strain-energy release rate calculated by the virtual crack extension method since the right hand side of this equation represents the energy change per unit crack extension [8]. Equation (13) is also equivalent to an equation obtained by de Lorenzi [6,7], by calculating the change in energy by mapping a crack configuration with a crack length of  $a$  to another crack configuration of length  $a + da$ .

Line Integrals — The four line integrals of Eq. (8) are

$$(J_{x_k})_{line} = \int_{FC} Q S d\Gamma + \int_{AD} Q S d\Gamma + \int_{CO} Q d\Gamma + \int_{OA} Q d\Gamma \quad (16)$$

When the term  $Q$  (defined by Eq. (2)) is zero on the crack faces, obviously, the line integrals are zero. On the crack faces,  $n_1$  is always zero; when the crack face is traction free,  $\sigma_{12}$  and  $\sigma_{22}$  are zero. Thus, for traction-free crack faces, the line integrals in  $J_{x_1}$  always vanish.

This is not the case with  $J_{x_2}$ , the product integral. The term  $Q$  contains the term  $Wn_2$ ;  $n_2 = -1$  on the line  $FO$  and  $n_2 = 1$  on the line  $OD$ . Thus, even for traction-free crack faces,  $Q$  (and line integral in  $J_{x_2}$ ) can be non-zero. If only mode *I* deformations exist, then the strain-energy density  $W$  is zero on lines  $FO$  and  $OD$ , and, thus,  $Q$  and the  $J_{x_2}$  line integrals are zero for traction-free crack faces. When mode *II* deformations occur and only the square-root singular term exists in the stress field, the sum of the integrals on  $FO$  and  $OD$  is zero due to the antisymmetric nature of the deformations, and again the  $J_{x_2}$  line integrals are zero. But in a general crack problem subjected to external loading, both singular and non-singular stress fields exist around the crack tip; thus, the  $J_{x_2}$  line integrals will be non-zero (see Appendix B for details). Evaluation of the line  $J_{x_2}$  integrals is complicated by the singular stress field and the strain-energy density at the crack

tip because of the line integrals on  $CO$  and  $OA$ . Thus, a method of calculating the mode  $I$  and mode  $II$  components in mixed mode problems, the decomposition method, in which the  $J_{x_2}$  line integrals vanish is presented in the next section.

### Separation of Modes in Mixed Mode Problems

Direct method — The two integrals  $J_{x_1}$  and  $J_{x_2}$  of Eq. (10) can be used to establish the individual modes. If  $J_I$  and  $J_{II}$  correspond to the pure mode  $I$  and pure mode  $II$  deformations, then [3,10]

$$\begin{aligned} J_{x_1} &= J_I + J_{II} \\ J_{x_2} &= -2\sqrt{J_I J_{II}} \end{aligned} \tag{17}$$

From Eq. (17),  $J_I$  and  $J_{II}$  can be computed in terms of  $J_{x_1}$  and  $J_{x_2}$  as

$$\begin{aligned} J_I &= \frac{1}{4} [ \sqrt{J_{x_1} - J_{x_2}} + \sqrt{J_{x_1} + J_{x_2}} ]^2 \\ J_{II} &= \frac{1}{4} [ \sqrt{J_{x_1} - J_{x_2}} - \sqrt{J_{x_1} + J_{x_2}} ]^2 \\ J_{total} &= J_I + J_{II} \end{aligned} \tag{18}$$

For general mixed mode deformation the computation of  $J_{x_1}$  and  $J_{x_2}$  from Eq. (13) and the use of Eqs. (17) and (18) completely define the individual modes. However, for either pure mode  $I$  or pure mode  $II$  deformations the values of  $J_{x_1}$  and  $J_{x_2}$  alone are insufficient to determine the individual modes. (Additional information such as the local crack tip deformation is needed to define the mode.) This is because in either case  $J_{x_2} \equiv 0$  and  $J_{x_1}$  gives the total integral. Equation (15) then suggests that only  $J_I$  exists. This difficulty is due to the choice of the positive sign for the square root terms in Eq. (18).

Decomposition method — As previously mentioned, the advantage of transforming the contour integral into a domain integral is lost because of the non-zero line integrals in  $J_{x_2}$ . These line integrals are necessary to account for the terms containing the product of the singular and non-singular stress (strain) fields in

the strain-energy density expression. It is shown in appendix B that the product terms can be eliminated by decomposing the stress and displacement fields into symmetric and antisymmetric parts. The resulting equation contains only the domain integral. This method termed as the decomposition method is described below.

Consider two points  $P(x_1, x_2)$  and  $P'(x_1, -x_2)$  that are in the immediate neighborhood of the crack tip and are symmetric about the crack line as shown in Figure 2. For general mixed mode deformations the displacements at  $P$  and  $P'$  can be expressed as a combination of symmetric and antisymmetric components as shown in Figure 2. Then

$$\begin{Bmatrix} u_{1P} \\ u_{2P} \end{Bmatrix} = \begin{Bmatrix} u_{1S} \\ u_{2S} \end{Bmatrix} + \begin{Bmatrix} u_{1AS} \\ u_{2AS} \end{Bmatrix} \quad (19)$$

and

$$\begin{Bmatrix} u_{1P'} \\ u_{2P'} \end{Bmatrix} = \begin{Bmatrix} u_{1S} \\ -u_{2S} \end{Bmatrix} + \begin{Bmatrix} -u_{1AS} \\ u_{2AS} \end{Bmatrix} \quad (20)$$

where subscripts  $S$  and  $AS$  denote the symmetric and antisymmetric components, respectively.

Equations (19) and (20) can be used to determine the symmetric and antisymmetric displacements in terms of the displacements at points  $P$  and  $P'$  (see Figure 2) as

$$\begin{Bmatrix} u_1 \\ u_2 \end{Bmatrix}_S = \frac{1}{2} \begin{Bmatrix} u_{1P} + u_{1P'} \\ u_{2P} - u_{2P'} \end{Bmatrix} \quad (21)$$

$$\begin{Bmatrix} u_1 \\ u_2 \end{Bmatrix}_{AS} = \frac{1}{2} \begin{Bmatrix} u_{1P} - u_{1P'} \\ u_{2P} + u_{2P'} \end{Bmatrix}$$

Similarly, the symmetric and antisymmetric components of the stresses can be expressed in terms of the stresses at points  $P$  and  $P'$  (see Figure 3) as

$$\begin{Bmatrix} \sigma_{11} \\ \sigma_{22} \\ \sigma_{12} \end{Bmatrix}_S = \frac{1}{2} \begin{Bmatrix} \sigma_{11P} + \sigma_{11P'} \\ \sigma_{22P} + \sigma_{22P'} \\ \sigma_{12P} - \sigma_{12P'} \end{Bmatrix} \quad (22)$$

$$\begin{Bmatrix} \sigma_{11} \\ \sigma_{22} \\ \sigma_{12} \end{Bmatrix}_{AS} = \frac{1}{2} \begin{Bmatrix} \sigma_{11P} - \sigma_{11P'} \\ \sigma_{22P} - \sigma_{22P'} \\ \sigma_{12P} + \sigma_{12P'} \end{Bmatrix}$$

The symmetric and antisymmetric displacements (Eq. (21)) and stresses (Eq. (22)) can be used to evaluate the four integrals  $J_{Sx_1}$ ,  $J_{Sx_2}$ ,  $J_{ASx_1}$ , and  $J_{ASx_2}$  using Eq. (10). Note that the integrals  $J_{Sx_2}$  and  $J_{ASx_2}$  (domain and line components individually) will be identically zero because of the symmetric and antisymmetric nature of the stress and displacement fields.

The individual modes,  $J_I$  and  $J_{II}$ , are now

$$\begin{aligned} J_I &= J_{Sx_1} \\ J_{II} &= J_{ASx_1} \\ J_{total} &= J_{Sx_1} + J_{ASx_1} \end{aligned} \quad (23)$$

Obviously, this procedure involves an additional step to evaluate the symmetric and antisymmetric components from Eqs. (21) and (22). However, the individual modes are directly available from the domain integrals  $J_{Sx_1}$  and  $J_{ASx_1}$ . For pure mode *I* problems  $J_{ASx_1} \equiv 0$  and  $J_{total} = J_{Sx_1}$ . For pure mode *II* problems  $J_{Sx_1} \equiv 0$  and  $J_{total} = J_{ASx_1}$ .

#### Crack-Face Pressure Loading

In the above discussion, the crack faces were assumed to be stress free. When the crack faces are subjected to applied loading, additional terms need to be included in the domain integral formulation.

Again consider equation (10)

$$J_{x_k} = (J_{x_k})_{domain} + (J_{x_k})_{line} \quad (10)$$

When the crack faces are loaded, the line integrals are (see Fig. 1(b))

$$\begin{aligned} (J_{x_k})_{line} &= \int_F^C [W n_k + \sigma_{12} \frac{\partial u_1}{\partial x_k} + \sigma_{22} \frac{\partial u_2}{\partial x_k}] S dx_1 \\ &+ \int_D^A [W n_k - \sigma_{12} \frac{\partial u_1}{\partial x_k} - \sigma_{22} \frac{\partial u_2}{\partial x_k}] S dx_1 \\ &+ \int_C^O [W n_k + \sigma_{12} \frac{\partial u_1}{\partial x_k} + \sigma_{22} \frac{\partial u_2}{\partial x_k}] dx_1 \\ &+ \int_A^O [W n_k - \sigma_{12} \frac{\partial u_1}{\partial x_k} - \sigma_{22} \frac{\partial u_2}{\partial x_k}] dx_1 \end{aligned} \quad (24)$$

In deriving Eq. (24),  $n_1 = 0$  and  $n_2 = 1$  were used on line  $AD$  and  $n_1 = 0$  and  $n_2 = -1$  were used on line  $FC$ . Note that when the crack faces are stress free  $\sigma_{12} = \sigma_{22} = 0$ . Therefore, all the line integrals vanish yielding only the domain integral of Eq. (10) as  $J_{x_k}$ .

For the decomposition method, the symmetric and antisymmetric line integrals  $J_{Sx_k}$  and  $J_{ASx_k}$  can be obtained by substituting the symmetric and antisymmetric components of stresses and displacements into Eq. (24). This yields

$$\begin{aligned} (J_{Sx_1})_{line} &= 2 \int_F^C \sigma_{22} \frac{\partial u_2}{\partial x_1} S dx_1 + 2 \int_C^O \sigma_{22} \frac{\partial u_2}{\partial x_1} dx_1 \\ (J_{Sx_2})_{line} &= 0 \\ (J_{ASx_1})_{line} &= 2 \int_F^C \sigma_{12} \frac{\partial u_1}{\partial x_1} S dx_1 + 2 \int_C^O \sigma_{12} \frac{\partial u_2}{\partial x_1} dx_1 \\ (J_{ASx_2})_{line} &= 0 \end{aligned} \quad (25)$$

**Case 1** – When the only loading on the crack faces is a uniform pressure of magnitude  $p$ ,

$$\sigma_{12} = 0 ; \sigma_{22} = -p \quad (26)$$

The symmetry of the deformation requires that

$$\left[ \frac{\partial u_2}{\partial x_1} \right]_{DA} = - \left[ \frac{\partial u_2}{\partial x_1} \right]_{FC}$$

and

$$\left[ \frac{\partial u_2}{\partial x_2} \right]_{DA} = \left[ \frac{\partial u_2}{\partial x_2} \right]_{FC} \quad (27)$$

Therefore, the line integrals reduce to

$$(J_{x_1})_{line} = (J_{Sx_1})_{line} = -2 \int_{-l_2}^{-l_1} p \frac{\partial u_2}{\partial x_1} S dx_1 - 2 \int_{-l_1}^0 p \frac{\partial u_2}{\partial x_1} dx_1 \quad (28)$$

$$(J_{x_2})_{line} = (J_{Sx_2})_{line} = (J_{ASx_1})_{line} = (J_{ASx_2})_{line} = 0$$

where  $(-l_2, 0)$  and  $(-l_1, 0)$  are the coordinates of points  $F$  and  $C$  in Fig. 1(b).

Case 2 – When the only loading on crack faces is a uniform shear of magnitude  $\tau$ ,

$$\sigma_{12} = \tau ; \sigma_{22} = 0 \quad (29)$$

The antisymmetry of deformation requires that

$$\left[ \frac{\partial u_1}{\partial x_1} \right]_{DA} = - \left[ \frac{\partial u_1}{\partial x_1} \right]_{FC}$$

and

$$\left[\frac{\partial u_1}{\partial x_2}\right]_{DA} = \left[\frac{\partial u_1}{\partial x_2}\right]_{FC} \quad (30)$$

Therefore, the line integrals reduce to

$$(J_{x_1})_{line} = (J_{AS_{x_1}})_{line} = 2 \int_{-l_2}^{-l_1} \tau \frac{\partial u_1}{\partial x_1} S dx_1 + 2 \int_{-l_1}^0 \tau \frac{\partial u_1}{\partial x_1} dx_1 \quad (31)$$

$$(J_{x_2})_{line} = (J_{S_{x_2}})_{line} = (J_{S_{x_1}})_{line} = (J_{AS_{x_2}})_{line} = 0$$

## RESULTS AND DISCUSSION

In this section, the EDI method is applied to two mode *I* problems and two mixed mode problems. Because only linear elastic materials are considered here, to validate the EDI method the *J*-domain integrals are compared to the strain-energy release rate values from the literature [14-18]. Unless otherwise specified, a Poisson's ratio of 0.3 was used for all configurations analyzed.

### Mode I problems

**Remote loading** – The first two examples considered are the center cracked tension (CCT) and single-edge cracked tension (SECT) specimens as shown in Figure 4(a) and (b), respectively. A crack-length-to-width ratio of 0.8 was considered. Due to the symmetries in the problems, either one-quarter or one-half of the specimen was modeled with 34 8-noded parabolic elements as shown in Figures 4(c) and (d). At the crack tip, collapsed quarter-point elements were used. Figure 5 shows the detail near the crack tip and also the domains  $D_1$ ,  $D_2$ , and  $D_3$  used to evaluate the domain integrals.

Figure 5 presents a variety of S-functions that were used in computing the domain integrals. Type I is a simple linear function. Types II and III are quadratic functions. These S-functions were created by defining the values of *S* at nodes on the elements, as discussed in appendix A. The functional forms corresponding to the S-functions are given in Figure A2. These three functions were used in conjunction with each of the domains  $D_1$ ,  $D_2$ , and  $D_3$ . The other two S-functions in Figure 5 involved two layers of elements, i.e., domains  $D_1$  and  $D_2$ , or  $D_2$  and

$D_3$ . These two functions were used to study the influence of using more than one layer of elements in the computation of the domain integrals.

Table 1 presents the normalized values of  $J_{x_1}$  ( $J_{Sx_1}$  and  $J_I$ ) obtained by considering various domains and S-functions for both CCT and SECT specimens. (Due to symmetry, the  $J_{x_1}$  values in this table correspond to twice the value computed with the elements in the various domains shown in Fig. 5. Also note that the  $J_{x_2}$  values computed from the elements in the domains  $D_i$  shown in Figure 5 were non-zero. However, the symmetric group of elements below the crack line contribute a value with the same magnitude but with opposite sign. Hence, the total value of  $J_{x_2}$  is equal to zero, as required by these mode I problems.) For comparison the normalized values of the strain-energy release rate  $G$  (and hence  $J_{x_1}$  or  $J_{Sx_1}$ ) from the literature [15-18] and obtained by the virtual crack closure technique (VCCT) [14] using the same finite element model are included in this table. For the CCT specimen, the various S-functions and domains give nearly identical results; the variation of the computed values was about 1.2 percent. For the SECT specimen, the domain integrals were nearly same with a maximum variation of 2 percent. The values computed using the EDI are, as expected, in excellent agreement with the VCCT calculations. The results in this table suggest that domains consisting of a single layer of elements and linear S-functions are sufficient to obtain accurate results.

The model in Figure 4(d) is locally symmetric about the crack tip. As mentioned previously, the finite element model need not be symmetric about a line normal to the crack line and parallel to the  $x_2$ -axis. To verify this, a new model without symmetry about the crack tip was developed. A simple rectangular idealization was used throughout the model as shown in Figure 6. Note that in this model singularity elements were not used at the crack tip. Three domains were used in the EDI calculations as shown in Figure 6. Linear S-functions were used in the EDI calculations. Table 2 presents the normalized values of  $J_{x_1}$  obtained with the three domains. All domains gave nearly identical results; the variation of the computed values was about 0.6 percent. Furthermore, these results agree extremely well with those calculated with quarter-point singularity elements at the crack tip and with the VCCT method. The normalized value of the integral with this model without singularity elements is about 3 percent lower than the value with singularity elements. Note that the application of the VCCT method is difficult when the finite-element model is not locally symmetric about the crack tip. The EDI method does not have such a restriction.

Crack-face loading — As pointed out earlier, the equivalent domain integrals need to be modified when the crack faces are subjected to external loading.

Consider the CCT specimen in Figure 4(a). Instead of the remote tensile loading shown, let the specimen be subjected a uniform crack-face pressure of magnitude  $p$ . Figure 7 presents the domains near the crack tip for one or two layers of elements. For each of the S-functions the line integrals in Eq. (28) were computed and are shown in Table 3.

Table 4 presents the domain and line components of the integrals  $J_{x_1}$  ( $J_{x_1} = J_{Sx_1} = J_I$ ) for the crack-face pressure loading. The sum of the domain and line components computed for the crack-face pressure loading is exactly equal to the domain integrals computed for the remote loading situation. This is true for all domains.

### Mixed Mode Problems

The second two examples considered are mixed mode problems, an angle crack problem (Fig. 8(a)) and a cracked bimaterial problem (Fig.8(b)). These problems are used to discuss the separation of individual modes using the domain integrals.

Angle crack – Figure 8(a) shows the configuration used for an angle crack in a finite plate. Figure 9(a) and (b) show the finite element idealization with 77 8-noded parabolic elements. At the crack tip, collapsed quarter-point elements were used.

Four domains  $D_1$  and  $D_2$  (Figure 9(b)) were used to evaluate the domain integrals. Three S-functions, Types I, II, and III, were used with the two domains. As mentioned previously,  $J_I$  and  $J_{II}$  can be evaluated by (a) computing  $J_{x_1}$  and  $J_{x_2}$  and using Eq. (18) or by (b) computing  $J_{Sx_k}$  and  $J_{ASx_k}$  and using Eq. (23). Table 5 presents the results obtained using both of these methods.

First, note that the total integral  $J_{x_1}$  is identically equal to the sum of  $J_{Sx_1}$  and  $J_{ASx_1}$ . Next, the integrals  $J_{Sx_1}$  ( $J_I$ ) and  $J_{ASx_1}$  ( $J_{II}$ ) agree very well with the  $J_I$  and  $J_{II}$  from the literature [14-18]. Third, the two domains and three S-functions showed a maximum variation of 0.3 percent for  $J_{Sx_1}$  and 1.5 percent for  $J_{ASx_1}$ . Thus  $J_{x_1}$  from the undecomposed displacement field and  $J_{Sx_1}$  and  $J_{ASx_1}$  from the symmetric and antisymmetric displacement fields yield accurate results.

The  $J_{II}$  values calculated using  $J_{x_1}$  and  $J_{x_2}$  are not accurate. The errors are in the calculation of the  $J_{x_2}$  integral. As previously mentioned,  $J_{x_2}$  includes the line integral in the singularity region and hence requires integration of singular terms near the crack tip. The line integrals in the singularity element region (i.e. in

quarter-point element region) were computed in the same manner as for non-singular elements, using a 2-point Gaussian quadrature. This may be the reason for about 3 percent error in the  $J$ -values in Table 5. When  $J_{x_2}$  was evaluated without including the line integrals very large errors were found and the results were domain dependent. Therefore, the line integrals are necessary for accurate evaluation of  $J_{x_2}$ .

The integrals  $J_{Sx_2}$  and  $J_{ASx_2}$  are also product integrals like  $J_{x_2}$ . These integrals were very nearly zero (within machine accuracy) for all domains and for all S-functions. Note that  $J_{Sx_2}$  ( $J_{ASx_2}$ ) was evaluated with the symmetric (antisymmetric) components of the displacements and stresses. Hence, the zero values computed for  $J_{Sx_2}$  and  $J_{ASx_2}$  were expected because of the symmetric and antisymmetric nature of the displacement field used in the computations. Also note that the line integral components are identically zero. From these results the decomposition method appears to be the preferable over the direct method (Eq. 18) to separate the modes.

Cracked bimaterial plate — The second mixed mode problem analyzed was a bimaterial plate with central crack along the interface (Fig. 8(b)). The plate was subjected to remote tensile loading. Different combinations of materials were used in the plate. The materials and their properties are summarized in Table 6. Because of symmetry, only one-half of the plate was idealized as shown in Fig. 10(a). Figure 10(b) shows the detail near the crack tip for a model with  $\frac{\Delta}{a}=0.05$ . This model had 517 nodes and 156 elements. At the crack tip, quarter-point singularity elements were used. Four domains and linear S-functions were used in the domain integral calculations.

In contrast to the angle crack problem where only the displacement field was decomposed into symmetric and antisymmetric components, in this problem both the displacements and the stress fields were decomposed. This was done because in the bimaterial problem, the stresses derived from a symmetric (or antisymmetric) displacement field yield both symmetric and antisymmetric (or antisymmetric and symmetric) stresses. The decomposed stresses and displacements were used to calculate the domain integrals.

Table 7 presents the integrals  $J_{Sx_1}$  and  $J_{ASx_1}$  for various combinations of materials and domains considered. These integrals are also compared to the strain-energy release rate calculated using VCCT formulae given in reference 13. First, note that the total integrals show less than one percent variation among the four domains for all material combinations. The total integrals also agree extremely well (within 1.6 percent) with the total strain-energy release rate calculated with

VCCT. Next, the mode *I* integrals show some variation among the four domains. The maximum variation between  $D_1$  and  $D_4$  is 4 percent for the aluminum-epoxy case, and is 4.8 percent for the steel-epoxy case. The differences between the mode *I* integral values of domain  $D_4$  and the VCCT values are 3, 3.4, and 0.2 percent for the aluminum-epoxy, steel-epoxy, and steel-aluminum combinations, respectively. The discrepancies are much smaller with other domains. In contrast to the total and the mode *I*, the mode *II* integrals show large variations among all the domains for all material combinations. (The variation of the mode *II*-to-total ratio is about 5 percent between the domains  $D_1$  and  $D_4$  for the steel-epoxy case.) Furthermore, the mode *II* integrals do not agree with those calculated with the VCCT. Also note that the discrepancies are much larger for the steel-epoxy case than the other material combinations.

The mode *I* and mode *II* domain dependence may be related to the oscillatory singularity that exists at the crack tip in a bimaterial plate [19]. The VCCT also yields inconsistent values of individual modes for different values of  $\Delta$ , the crack closure length [19]. To determine the effect of  $\Delta$ , the crack-tip singularity element size was reduced from  $\frac{\Delta}{a} = 0.05$  to 0.025. The new model with  $\frac{\Delta}{a} = 0.025$  is shown in Fig. 10(c). This model was obtained by subdividing each of the 8 singularity elements into two elements; a regular 8-noded element and a singularity element. This new model had 543 nodes and 164 elements. Five domains were used with this new model but the domains  $D_1$  to  $D_4$  were the same as the model of Fig 10(b). Because the steel-epoxy has the largest differences in the material properties (and hence the largest oscillatory power), the steel-epoxy case was analyzed with this new model.

Table 8 presents the mode *I*, mode *II*, and total integrals obtained with various domains and with the two models of Figs. 10(b) and 10(c). The results from the two models are almost identical for domains  $D_1$  to  $D_4$ . The total integral for domain  $D_5$  is only different by 0.3 percent when compared to that of domain  $D_4$ . Thus, the model with  $\frac{\Delta}{a} = 0.025$  shows the same domain dependence of the mode *I* and mode *II* values. The mode *I* and mode *II* VCCT results, as expected, also show a dependence on  $\Delta$ , the crack closure length. In contrast, the total strain-energy release rate is virtually unchanged as  $\frac{\Delta}{a}$  is reduced from 0.05 to 0.025. As shown in reference 19, the mode *I* and mode *II* strain-energy release rates do not have well defined limits as  $\Delta$  approaches zero. However, the total strain-energy release rate is independent of  $\Delta$ . This is exactly the behavior displayed here by the *J*-integrals. Therefore, the inconsistent behavior of mode *I* and mode *II* integrals is due to the oscillatory singularity. The different domains correspond to different values of  $\Delta$  in the VCCT. Hence, the domains  $D_1$ ,  $D_2$ , etc. show a continuously changing value of mode *I* and mode *II* while the total *J* remains

unchanged. Thus, the EDI method and VCCT are consistent and are simply reflecting the continuum behavior.

## CONCLUDING REMARKS

An equivalent domain integral (EDI) method for the calculation of  $J$ -integral fracture parameters (total and product integrals) is presented for two-dimensional elastic cracked bodies. The integrals consist of an area or domain and line integrals on the crack faces. The line integrals vanish only when the crack faces are traction free and the loading is either pure mode  $I$  or pure mode  $II$  or a combination of both with only the square-root singular term in the stress field. However, for finite size crack bodies subjected to mixed mode loading, even when the crack faces are traction free, the line integrals on the crack faces are non zero and are necessary to account for the non-singular field. Two methods for calculating the  $J$ -domain integrals for individual modes are discussed.

The EDI method gave accurate values of the  $J$ -integrals for the various mode  $I$  and mixed mode problems studied. The calculated integrals agreed very well with the strain-energy release rates from the literature. The numerical studies showed that domains consisting of one layer of finite elements were sufficient to give accurate results. Several types of S-functions, the functions that facilitate the conversion of the line  $J$ -integrals to the domain integrals, were used in the numerical studies. These studies showed that the results are independent of the type of S-functions studied and even the use of simple linear S-functions yields accurate results.

Two methods, direct and decomposition, for evaluating the individual mode components were studied. In the direct method the total and product  $J$ -integrals are computed and the individual modes are calculated from these two integral values. In the decomposition method, the displacements and stresses are first decomposed into the symmetric and antisymmetric components and then the  $J$ -integrals are evaluated for each of these components. The decomposition method was found to be more accurate than the decomposition method. The direct method requires evaluation of line integrals on the crack faces and hence requires integration of singular strain energy density near the crack tip. Numerical integration of these terms contributed to the loss of accuracy in this method. In contrast the line components are identically zero in the decomposition method.

For cracks in a homogeneous material only the displacement field needs to be decomposed into the symmetric and antisymmetric components. On the other hand, for bimaterial plates with cracks along the interface both the displacement

and stress fields need to be decomposed. For a bimaterial specimen the domain integrals calculated with the decomposed displacement and stress fields produce mode *I* and mode *II* *J*-integral values that show domain dependence in a manner similar to the dependence on the crack closure length in the virtual crack closure technique (VCCT). This behavior is caused by the oscillatory part of the singularity in the bimaterial crack problem. However, the total *J*-integral is domain independent.

## REFERENCES

- [1] J. D. Eshelby, " The continuum theory of lattice defects," *Solid State Physics*, F. Seitz and D. Turnbull, Eds., Vol. III, Academic Press, New York, 1966, pp. 79-144.
- [2] J. R. Rice, " A path-independent integral and the approximate analyses of strain concentration by notches and cracks," *J. Appl. Mech.*, Vol. 35, 1968, pp. 376-386.
- [3] G. P. Cherapanov, *Mechanics of Brittle Fracture*, Translated and Edited by R. W. De Wit and W. C. Cooley, McGraw Hill, New York, 1979.
- [4] D. M. Parks, " A stiffness derivative finite element technique for determination of crack tip stress intensity factors," *Int. Jnl. Fracture*, Vol. 10, 1974, pp. 487-502.
- [5] T. K. Hellen, " On the method of virtual crack extension," *Int. Jnl. Numer. Methods in Engng.*, Vol. 9, 1975, pp. 187-207.
- [6] H. G. de Lorenzi, " On energy release rate and the  $J$ -integral for 3-D crack configuration," *Int. Jnl. of Fracture*, Vol. 19, 1982, pp. 183-192.
- [7] H. G. de Lorenzi, " Energy release rate calculations by the finite element method," *Engng. Fract. Mech.*, Vol. 21, 1985, pp. 129-143.
- [8] F. Z. Li, C. F. Shih, and A. Needleman, " A comparison of methods for calculating energy release rates," *Engng. Fract. Mech.*, Vol. 21, 1985, pp. 405-421.
- [9] N. Miyakazi, T. Watanabe and G. Yagawa, " The virtual crack extension for evaluation of  $J$ - and  $\hat{J}$ -integrals," *Engng. Fract. Mech.*, Vol. 22, 1985, pp. 975- 987.
- [10] G. P. Nikishkov and S. N. Atluri, " An equivalent domain integral method for computing crack-tip integral parameters in non-elastic, thermo-mechanical fracture," *Engng. Fract. Mech.*, Vol. 26, 1987, pp. 851-867.
- [11] G. P. Nikishkov and S. N. Atluri, " Calculation of fracture mechanics parameters for an arbitrary three-dimensional crack, by the 'equivalent domain integral' method," *Int. Jnl. Numer. Methods in Engng.*, Vol. 24, 1987, pp. 1801-1821.

- [12] I. S. Raju and J. C. Newman, Jr., " Stress-intensity factors for a wide range of semi-elliptical surface cracks in finite-thickness plates," *Engng. Fract. Mech.*, Vol. 11, 1979, pp. 817-829.
- [13] K. N. Shivakumar, P. W. Tan, and J. C. Newman, Jr., " A Virtual Crack Closure Technique for Calculating Stress-Intensity Factors for Cracked Three-Dimensional Bodies," *Int. Jnl. Fract.*, Vol. 36, 1988, pp. R43-R50.
- [14] I. S. Raju, " Calculation of strain-energy release rates with higher order and singular finite elements," *Engng. Fract. Mech.*, Vol. 28, 1987, pp. 251-274.
- [15] H. Tada, P. C. Paris, and G. R. Irwin, *The Stress Analysis of Cracks Handbook*, Del Research Corp., St. Louis, 1973.
- [16] D. P. Rooke and D. J. Cartwright, *Compendium of Stress-Intensity Factors*, HMSO, London, 1976.
- [17] Y. Murakami et. al. (Eds), *Stress Intensity Factors Handbook*, Volumes 1 and 2, Pergamon Press, Tokyo, 1987.
- [18] P. W. Tan, I. S. Raju, and J. C. Newman, Jr., " Boundary force method for analyzing two-dimensional cracked plates," *Fracture Mechanics: Eighteenth Symposium, ASTM STP 945*, D. T. Read and R. P. Reed, Eds., American Society for Testing and Materials, Philadelphia, 1988, pp. 259-277. (NASA TM-87725, May, 1985).
- [19] I. S. Raju, J. H. Crews, Jr., and M. A. Aminpour, " Convergence of strain-energy-release rate components for edge-delaminated composite laminates," *Engng. Fract. Mech.*, Vol. 30, 1988, pp. 383-396.

## APPENDIX A NUMERICAL IMPLEMENTATION OF THE EDI METHOD

This appendix presents the numerical implementation of the EDI method in the context of a finite element analysis with isoparametric elements. Some of the details presented in this appendix can also be found in references 8,10, and 11.

A typical finite element model with 8-noded isoparametric elements that is locally symmetric about the crack line ( $x_2 = 0$ ) is shown in Figure A1. This type of locally symmetric model is necessary for the computation of  $J_{Sx_1}$ ,  $J_{ASx_1}$ , etc. (Eq. (19-22)). In contrast, either symmetric or non-symmetric models can be used if  $J_{x_1}$  and  $J_{x_2}$  are to be computed. Note that symmetry of the model with respect to the  $x_1 = 0$  line is not a requirement.

Consider the two contours  $\Gamma_0$  and  $\Gamma_1$  that constitute one layer of elements as shown in Figure A1. More than one layer of elements may be considered. However, one layer is considered here for convenience in presentation. As is shown in the results and discussion section, the results do not depend on the number of layers of elements between  $\Gamma_0$  and  $\Gamma_1$  and one layer of elements is computationally very convenient.

The elements I, J, K, L, L', K', J', and I' are bound by the contours  $\Gamma_0$  and  $\Gamma_1$ . Thus the domain integral is

$$(J_{x_k})_{domain} = \sum_i^{I, J, \dots, I'} J_{x_{k_i}} \quad (A1)$$

where  $J_{x_{k_i}}$  is the area integral over the  $i^{th}$  element.

In the isoparametric representation, the displacements within the element are defined by the shape functions  $N_j$  and the nodal displacements  $(u_\alpha)_j$

$$u_\alpha = N_j(u_\alpha)_j \quad (A2)$$

where  $\alpha = 1, 2$ ,  $N_j = N_j(\xi, \eta)$ ,  $\xi, \eta$  are the parent coordinates and  $j = 1$  to the number of nodes on the element.

The area integral  $J_{x_{k_i}}$  of the  $i^{th}$  element, Eq. (13), can be computed using Gaussian quadrature as

$$\begin{aligned}
(J_{x_{k_i}})_{domain} &= - \left[ \int_{-1}^1 \int_{-1}^1 \left[ W \frac{\partial S}{\partial x_k} - \{u'_{x_k}\}^T [\underline{\sigma}] \{S'\} \right] (det [\mathbf{J}]) d\xi d\eta \right. \\
&\quad \left. + \int_{-1}^1 \int_{-1}^1 \left[ \frac{\partial W}{\partial x_k} - \{\sigma\}^T \{\epsilon'_{x_k}\} \right] S (det [\mathbf{J}]) d\xi d\eta \right]_i \\
&= - \left[ \sum_{m=1}^{M_G} \sum_{n=1}^{M_G} \left\{ \left[ W \frac{\partial S}{\partial x_k} - \{u'_{x_k}\}^T [\underline{\sigma}] \{S'\} \right] \right. \right. \\
&\quad \left. \left. + \left[ \frac{\partial W}{\partial x_k} - \{\sigma\}^T \{\epsilon'_{x_k}\} \right] S \right\} w_m w_n (det[\mathbf{J}]) \right]_i
\end{aligned} \tag{A3}$$

where  $M_G$  is the number of Gaussian quadrature points used in each direction  $\xi$  and  $\eta$ ,  $w_m$  and  $w_n$  are the Gaussian weights and  $det [\mathbf{J}]$  is the determinant of the Jacobian matrix  $[\mathbf{J}]$  defined by

$$[\mathbf{J}] = \begin{bmatrix} \frac{\partial N_1}{\partial \xi} & \frac{\partial N_2}{\partial \xi} & \dots & \frac{\partial N_8}{\partial \xi} \\ \frac{\partial N_1}{\partial \eta} & \frac{\partial N_2}{\partial \eta} & \dots & \frac{\partial N_8}{\partial \eta} \end{bmatrix} \begin{bmatrix} (x_1)_1 & (x_2)_1 \\ (x_1)_2 & (x_2)_2 \\ \cdot & \cdot \\ \cdot & \cdot \\ \cdot & \cdot \\ (x_1)_8 & (x_2)_8 \end{bmatrix} \tag{A4}$$

Most of the quantities necessary for Eqs. (13-15),  $W$ ,  $\{\sigma\}$ ,  $\{\epsilon'_{x_k}\}$ ,  $\{u'_{x_k}\}$ , and  $[\underline{\sigma}]$ , are readily known in terms of the nodal displacements of the element. However, computation of the terms  $S$ ,  $\{S'\}$ , and  $\frac{\partial W}{\partial x_k}$  needs special attention and is discussed below.

**S-Functions** — As mentioned previously, the S-function needs to be continuous and have values equal to zero on the contour  $\Gamma_1$  and unity on the contour  $\Gamma_0$ . The S-function can be conveniently defined using the element shape functions as

$$S(\xi, \eta) = N_j S_j \quad (A5)$$

where  $j = 1$  to the number of nodes on the element and  $S_j$  is the nodal value of the S-function at node  $j$  on the element. The requirement that the function be zero on  $\Gamma_1$  and unity on  $\Gamma_0$  can be satisfied by specifying zero values for  $S$  at nodes 1, 8, and 7 on the  $\eta = 1$  line and unit values at nodes 3, 4, and 5 on the  $\eta = -1$  line of the parent element (see Figure A1). All values of  $S_j$  except those at the midside nodes 2 and 6 are now defined. Various choices of  $S_j$  for nodes 2 and 6 lead to different types of S-functions and these are illustrated in Figure A2. Thus specifying the nodal values  $S_j$  completely defines the S-functions. In fact a single subprogram that defines the nodal values  $S_j$  and, hence, the S-function can be used for all elements between  $\Gamma_0$  and  $\Gamma_1$ . The only requirement for all elements I, J, . . . I' is that the lines with  $\eta = -1$  should correspond to the contour  $\Gamma_0$  and the lines with  $\eta = 1$  should correspond to the contour  $\Gamma_1$  ( see elements K and K' in Fig. A2). This can be achieved by defining the element connectivity appropriately.

Partial Derivatives of S – Once  $S$  is defined the partial derivatives of  $S$ ,  $\frac{\partial S}{\partial x_1}$  and  $\frac{\partial S}{\partial x_2}$ , can be easily computed using the isoparametric formulation as

$$\begin{Bmatrix} \frac{\partial S}{\partial x_1} \\ \frac{\partial S}{\partial x_2} \end{Bmatrix} = [J]^{-1} \begin{Bmatrix} \frac{\partial S}{\partial \xi} \\ \frac{\partial S}{\partial \eta} \end{Bmatrix} \quad (A6)$$

where  $[J]$  is the Jacobian matrix defined in Eq. (A4).

Partial Derivatives of W – The terms  $\frac{\partial W}{\partial x_k}$  are computed using a bilinear extrapolation (in terms of the parent coordinates  $\xi$  and  $\eta$ ) for  $W$  and using the values of  $W$  at the  $2 \times 2$  integration points. In reference 10, the integral  $\int \frac{\partial W}{\partial x_k} dA$  was approximated with a one-point integration by evaluating  $\frac{\partial W}{\partial x_k}$  at the center of the element. A slightly different approach is taken here. Because all the quantities are known at the integration points, the integration is carried out in the same manner, without further approximations, as for the other terms in Eq. (13). The values of the stresses are known to be more reliable at the  $2 \times 2$  Gaussian points within the element (in comparison to the nodal values). The strain- energy density  $W$  is approximated in the bilinear form as

$$W(\xi, \eta) = a_1 + a_2 \xi + a_3 \eta + a_4 \xi \eta \quad (A7)$$

Using the 2 x 2 Gaussian values of the strain-energy density  $W$ , Eq. (A7) can be rewritten as

$$W(\xi, \eta) = [1 \quad \xi \quad \eta \quad \xi\eta] [T] \{W_G\} \quad (A8)$$

where

$$[T] = \frac{1}{4} \begin{bmatrix} 1 & 1 & 1 & 1 \\ -\sqrt{3} & -\sqrt{3} & \sqrt{3} & \sqrt{3} \\ -\sqrt{3} & \sqrt{3} & -\sqrt{3} & \sqrt{3} \\ 3 & -3 & -3 & 3 \end{bmatrix} \quad (A9)$$

and

$$\{W_G\}^T = \{W_I \quad W_{II} \quad W_{III} \quad W_{IV}\}^T \quad (A10)$$

$W_I, W_{II}, W_{III}$ , and  $W_{IV}$  are the values of  $W$  at the 2 x 2 Gaussian points shown in Figure A3. The partial derivatives  $\frac{\partial W}{\partial \xi}$  and  $\frac{\partial W}{\partial \eta}$  are

$$\begin{Bmatrix} \frac{\partial W}{\partial \xi} \\ \frac{\partial W}{\partial \eta} \end{Bmatrix} = \begin{bmatrix} 0 & 1 & 0 & \eta \\ 0 & 0 & 1 & \xi \end{bmatrix} [T] [W_G] \quad (A11)$$

Equation (A11) simplifies considerably and can be rewritten as

$$\frac{\partial W}{\partial \xi} = -\frac{\sqrt{3}}{4} (W_I + W_{II} - W_{III} - W_{IV}) + \frac{3\eta}{4} (W_I - W_{II} - W_{III} + W_{IV})$$

$$\frac{\partial W}{\partial \eta} = -\frac{\sqrt{3}}{4} (W_I - W_{II} + W_{III} - W_{IV}) + \frac{3\xi}{4} (W_I - W_{II} - W_{III} + W_{IV}) \quad (A12)$$

The derivatives  $\frac{\partial W}{\partial x_k}$  can now be obtained as

$$\begin{Bmatrix} \frac{\partial W}{\partial x_1} \\ \frac{\partial W}{\partial x_2} \end{Bmatrix} = [\mathbf{J}]^{-1} \begin{Bmatrix} \frac{\partial W}{\partial \xi} \\ \frac{\partial W}{\partial \eta} \end{Bmatrix} \quad (A13)$$

where  $[\mathbf{J}]$  is defined in Eq. (A4).

All the necessary quantities in Eq. (13) are now known and, hence, the domain integrals can be calculated.

## APPENDIX B

### NONSINGULAR STRESS FIELD IN THE COMPUTATION OF $(J_{x_2})_{line}$ INTEGRALS

This appendix examines the  $(J_{x_2})_{line}$  integrals when both the singular and nonsingular terms exist in the stress field. This appendix shows that line integrals vanish when the decomposition method is used.

For the purpose of this discussion consider a 2-D cracked body subjected to a mixed-mode stress field ( $K_I$  and  $K_{II}$ ) along with a uniform stress,  $\sigma_{11} = \sigma_0$ . The stresses along the two crack faces  $FO$  and  $DO$  (see Figure 1(b)) can be written in terms of the polar coordinates  $(r, \theta)$  with the origin at the crack tip as [15]

$$\sigma_{11} = \frac{-2 K_{II}}{\sqrt{2 \pi r}} + \sigma_0 \quad (B1)$$

on  $FO$  and

$$\sigma_{11} = \frac{2 K_{II}}{\sqrt{2 \pi r}} + \sigma_0 \quad (B2)$$

on  $DO$ . The stresses  $\sigma_{22}$  and  $\sigma_{12}$  are identically zero on both  $FO$  and  $DO$  since the crack faces are stress free. Also note that the mode  $I$  stress field does not contribute to the  $\sigma_{11}$  stresses on either  $FO$  or  $DO$ . Assuming plane strain conditions, strains  $\epsilon_{11}$  are

$$\epsilon_{11} = \frac{(1 - \nu^2)}{E} \left[ \frac{-2 K_{II}}{\sqrt{2 \pi r}} + \sigma_0 \right] \quad (B3)$$

on  $FO$  and

$$\epsilon_{11} = \frac{(1 - \nu^2)}{E} \left[ \frac{2 K_{II}}{\sqrt{2 \pi r}} + \sigma_0 \right] \quad (B4)$$

on  $DO$ .

For traction-free crack face problems  $Q$ , see equation (2), reduces to

$$Q = W n_k = \frac{1}{2} \sigma_{11} \epsilon_{11} n_k \quad (B5)$$

where  $W$  is the strain energy density and  $n_k$  is the component of the vector normal to the crack face in the  $k^{th}$  direction.

The line integrals corresponding to  $J_{x_1}$  vanish because  $n_1 = 0$  on  $FO$  and  $OD$  and hence  $Q$  is identically zero. Therefore, only the  $(J_{x_2})_{line}$  integral needs to be examined. Using Eqs. (B1) - (B5) and assuming that  $CO = OA$ , and  $FC = DA$ , the  $(J_{x_2})_{line}$  integral can be written as

$$\begin{aligned} \frac{2E J_{x_2 line}}{(1 - \nu^2)} = & - \int_{r_F}^{r_C} \left( \sigma_0 - \frac{2K_{II}}{\sqrt{2\pi r}} \right)^2 S dr + \int_{r_A}^{r_D} \left( \sigma_0 + \frac{2K_{II}}{\sqrt{2\pi r}} \right)^2 S dr \\ & - \int_{r_C}^O \left( \sigma_0 - \frac{2K_{II}}{\sqrt{2\pi r}} \right)^2 S dr + \int_O^{r_A} \left( \sigma_0 + \frac{2K_{II}}{\sqrt{2\pi r}} \right)^2 S dr \end{aligned} \quad (B6)$$

where  $r_F = r_D = l_2$  and  $r_C = r_A = l_1$ . Note that  $(-l_2, 0)$  and  $(-l_1, 0)$  are the coordinates of the points  $F$  and  $C$  in Figure 1(b). The line integral of Eq. (B6) simplifies to

$$(J_{x_2})_{line} = \frac{4(1 - \nu^2)}{E} \sigma_0 K_{II} \left[ \int_{r_C}^{r_F} \frac{S}{\sqrt{2\pi r}} dr + \int_O^{r_C} \frac{1}{\sqrt{2\pi r}} dr \right] \quad (B7)$$

The contributions in Eq. (B7) are due to the product of singular ( $K_{II}$ ) and nonsingular ( $\sigma_0$ ) terms. If only a pure singular stress field exists in the cracked body (i.e., when  $\sigma_0 = 0$ ), then the  $(J_{x_2})_{line}$  is identically equal to zero. Therefore, the presence of a nonsingular stress field in a mixed-mode problem gives a non zero  $(J_{x_2})_{line}$  integral. Numerical evaluation of this integral is difficult near the crack tip due to  $1/\sqrt{r}$  singularity (see Eq. B7).

Using the decomposition method, the symmetric and antisymmetric stress fields along the crack faces can be written as

Symmetric :

$$(\sigma_{11})_{Singular} = 0$$

(B11)

$$(\sigma_{11})_{Nonsingular} = \sigma_0$$

Antisymmetric :

$$(\sigma_{11})_{Singular} = \frac{-2 K_{II}}{\sqrt{2 \pi r}}$$

(B12)

$$(\sigma_{11})_{Nonsingular} = 0$$

Note that the product of singular and nonsingular terms for both symmetric and antisymmetric stress fields is identically zero. From Eq. (B7), it is obvious that the line integrals for conditions (B8) and (B9) vanish separately. Because the decomposition method considers symmetric and antisymmetric components separately, their cross terms are eliminated. Thus,  $(J_{Sx_2}$  and  $J_{ASx_2})$  line integrals are identically equal to zero.

**Table 1** Comparison of non-dimensional J-integral for CCT and SECT specimens subjected to remote tensile loading. (Plane strain,  $\frac{a}{b} = 0.8$ )

Domain	S-Function	$\frac{EJ_{x_1}}{p^2 \pi a (1-\nu^2)}$	
		CCT	SECT
$D_1$	Type I	3.285	137.1
$D_2$		3.284	136.7
$D_3$		3.283	137.1
$D_1$	Type II	3.274	135.8
$D_2$		3.273	136.4
$D_3$		3.270	137.0
$D_1$	Type III	3.297	138.4
$D_2$		3.295	137.0
$D_3$		3.296	137.2
$D_1 \& D_2$	Type IV	3.302	137.0
$D_2 \& D_3$		3.309	136.6
$D_1 \& D_2$	Type V	3.290	135.7
$D_2 \& D_3$		3.298	136.3
VCCT [14]		3.396	137.4
Reference Value [15-17]		3.298	143.8

**Table 2** Comparison of non-dimensional J-integral for CCT specimen subjected to remote tensile loading computed with a model with non-singular elements. (Figure 6, Plane strain,  $\frac{a}{b} = 0.8$ )

Domain	$\frac{EJ_{z1}}{p^2\pi a(1-\nu^2)}$
$D_1$	3.201
$D_2$	3.221
$D_3$	3.219

**Table 3** Line integrals for various S-functions (see Figure 7)

One layer of elements in the domain	
S-Function	Line-integrals $(J_{x1})_{line}$ and $(J_{Sx1})_{line}$
Type I $(S_i = 1, S_j = 0.5, S_k = 0)$	$\frac{2p}{6}[u_{2i} + 4u_{2j} + u_{2k}]$
Type II $(S_i = 1, S_j = S_k = 0)$	$\frac{2p}{6}[3u_{2i} + 4u_{2j} - u_{2k}]$
Type III $(S_i = S_j = 1, S_k = 0)$	$\frac{2p}{6}[-u_{2i} + 4u_{2j} + 3u_{2k}]$
Two layers of elements in the domain	
Type IV $(S_i = S_j = S_k = 1, S_l = 0.5, S_m = 0)$	$\frac{2p}{6}[u_{2k} + 4u_{2l} + u_{2m}]$
Type V $(S_i = S_j = S_k = 1, S_l = S_m = 0)$	$\frac{2p}{6}[3u_{2k} + 4u_{2l} - u_{2m}]$

**Table 4** Comparison of non-dimensional J-integral for crack face pressure and remote loadings for the CCT specimen. (Plane strain,  $\frac{a}{b} = 0.8$ )

Domain	S-Function	$\frac{EJ_{x_1}}{p^2 \pi a (1-\nu^2)}$			
		Crack face pressure loading			Remote loading
		$(J_{x_1})_{domain}$	$(J_{x_1})_{line}$	$(J_{x_1})_{total}$	$(J_{x_1})_{domain}$
$D_1$	Type I	1.872	1.413	3.285	3.285
$D_2$		2.064	1.220	3.284	3.284
$D_3$		2.322	0.961	3.283	3.283
$D_1$	Type II	1.916	1.357	3.273	3.273
$D_2$		2.127	1.146	3.273	3.273
$D_3$		2.412	0.858	3.270	3.270
$D_1$	Type III	1.828	1.469	3.297	3.297
$D_2$		2.001	1.294	3.295	3.295
$D_3$		2.233	1.063	3.296	3.296
$D_1 \& D_2$	Type IV	1.889	1.413	3.302	3.302
$D_2 \& D_3$		2.089	1.220	3.309	3.309
$D_1 \& D_2$	Type V	1.933	1.357	3.290	3.290
$D_2 \& D_3$		2.152	1.146	3.298	3.298

**Table 5** Comparison of  $\frac{EJ}{[p^2\pi a(1-\nu^2)]}$  computed from direct and decomposition methods for an angle crack problem. (Figure 7, Plane strain,  $\frac{a}{b} = 0.5, \phi = 45^\circ$ )

Domain	S-Function	Direct method				Decomposition	Method
		$J_{x_1}$	$J_{x_2}$	$J_I$	$J_{II}$	$J_{Sx_1}(J_I)$	$J_{ASx_1}(J_{II})$
$D_1$	Type I	1.781	-1.317	1.489	0.291	1.439	0.342
$D_2$		1.774	-1.304	1.481	0.293	1.437	0.338
$D_3$		1.775	-1.320	1.481	0.294	1.437	0.338
$D_4$		1.775	-1.324	1.478	0.296	1.437	0.338
$D_1$	Type II	1.781	-1.320	1.488	0.293	1.440	0.341
$D_2$		1.774	-1.318	1.480	0.294	1.436	0.338
$D_3$		1.774	-1.320	1.479	0.294	1.436	0.338
$D_4$		1.770	-1.321	1.474	0.296	1.432	0.338
$D_1$	Type III	1.780	-1.314	1.491	0.290	1.438	0.343
$D_2$		1.775	-1.318	1.482	0.293	1.437	0.338
$D_3$		1.776	-1.320	1.482	0.294	1.438	0.338
$D_4$		1.779	-1.326	1.482	0.297	1.441	0.338
				VCCT	[14]	1.447	0.340
				Collocation	[15-17]	1.440	0.325
				BFM	[18]	1.416	0.330

**Table 6** Material properties used in the bimaterial plate problems.

Material	E, psi	$\nu$
Epoxy	$0.45 \times 10^6$	0.35
Aluminum	$10.0 \times 10^6$	0.30
Steel	$30.0 \times 10^6$	0.30

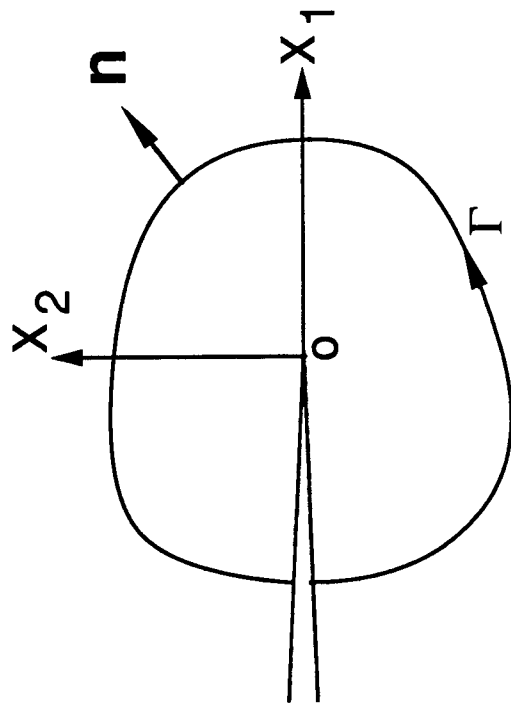
**Table 7** Comparison of the non-dimensional J-integral for a center cracked bi-material plate subjected to remote tensile loading. (Plane strain,  $\frac{a}{b} = 0.1$ )

Material		Domain	$\frac{E_1 J}{p^2 \pi a (1 - \nu_1^2)}$		
1	2		Mode I	Mode II	Total
Aluminum	Aluminum	$D_1$	1.012	0.0	1.012
		$D_2$	1.012	0.0	1.012
		$D_3$	1.012	0.0	1.012
		$D_4$	1.012	0.0	1.012
			(1.010)*	(0.0)	(1.010)
Aluminum	Epoxy	$D_1$	8.771	0.590	9.361
		$D_2$	8.659	0.716	9.375
		$D_3$	8.571	0.807	9.378
		$D_4$	8.426	0.989	9.415
			(8.671)	(0.613)	(9.284)
Steel	Epoxy	$D_1$	24.44	1.924	26.37
		$D_2$	24.09	2.329	26.41
		$D_3$	23.81	2.618	26.42
		$D_4$	23.34	3.204	26.54
			(24.13)	(1.996)	(26.13)
Steel	Aluminum	$D_1$	1.893	0.0333	1.931
		$D_2$	1.885	0.0467	1.931
		$D_3$	1.875	0.0567	1.932
		$D_4$	1.859	0.0750	1.934
			(1.863)	(0.0581)	(1.921)

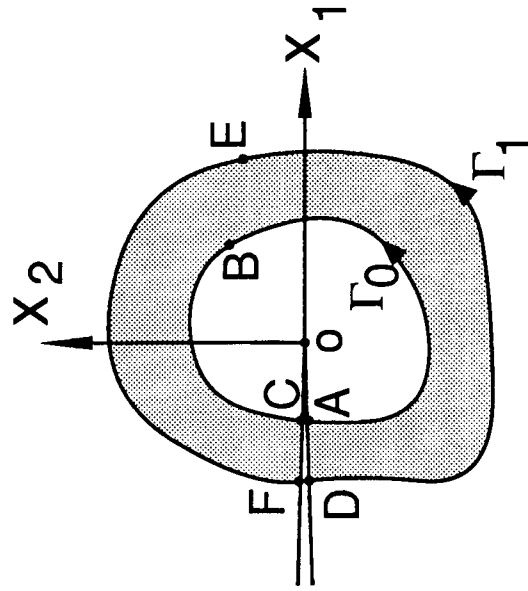
**Table 8** Comparison of the non-dimensional J-integral for a center cracked steel-epoxy bi-material plate subjected to remote tensile loading for two values of  $(\Delta/a) = 0.05$  and  $0.025$ . (Figure 8, Plane strain,  $\frac{a}{b} = 0.1$ )

$\frac{\Delta}{a}$	Domain	$\frac{E_1 J}{p^2 \pi a (1 - \nu_1^2)}$		
		Mode I	Mode II	Total
0.05	$D_1$	24.44	1.924	26.37
	$D_2$	24.09	2.329	26.41
	$D_3$	23.81	2.618	26.42
	$D_4$	23.34	3.204	26.54
	VCCT	(24.13)*	(1.996)	(26.13)
0.025	$D_1$	24.44	1.924	26.37
	$D_2$	24.09	2.325	26.42
	$D_3$	23.81	2.614	26.42
	$D_4$	23.31	3.228	26.53
	$D_5$	22.62	3.983	26.61
	VCCT	(23.43)	(2.765)	(26.19)

\* Values in the parentheses were obtained with VCCT formulae given in reference 14.



(a) Coordinate system and contour  $\Gamma$  around the crack tip.



(b) Domain bounded by contours  $\Gamma_0$  and  $\Gamma_1$ .

Figure 1 - Contours around the crack tip.

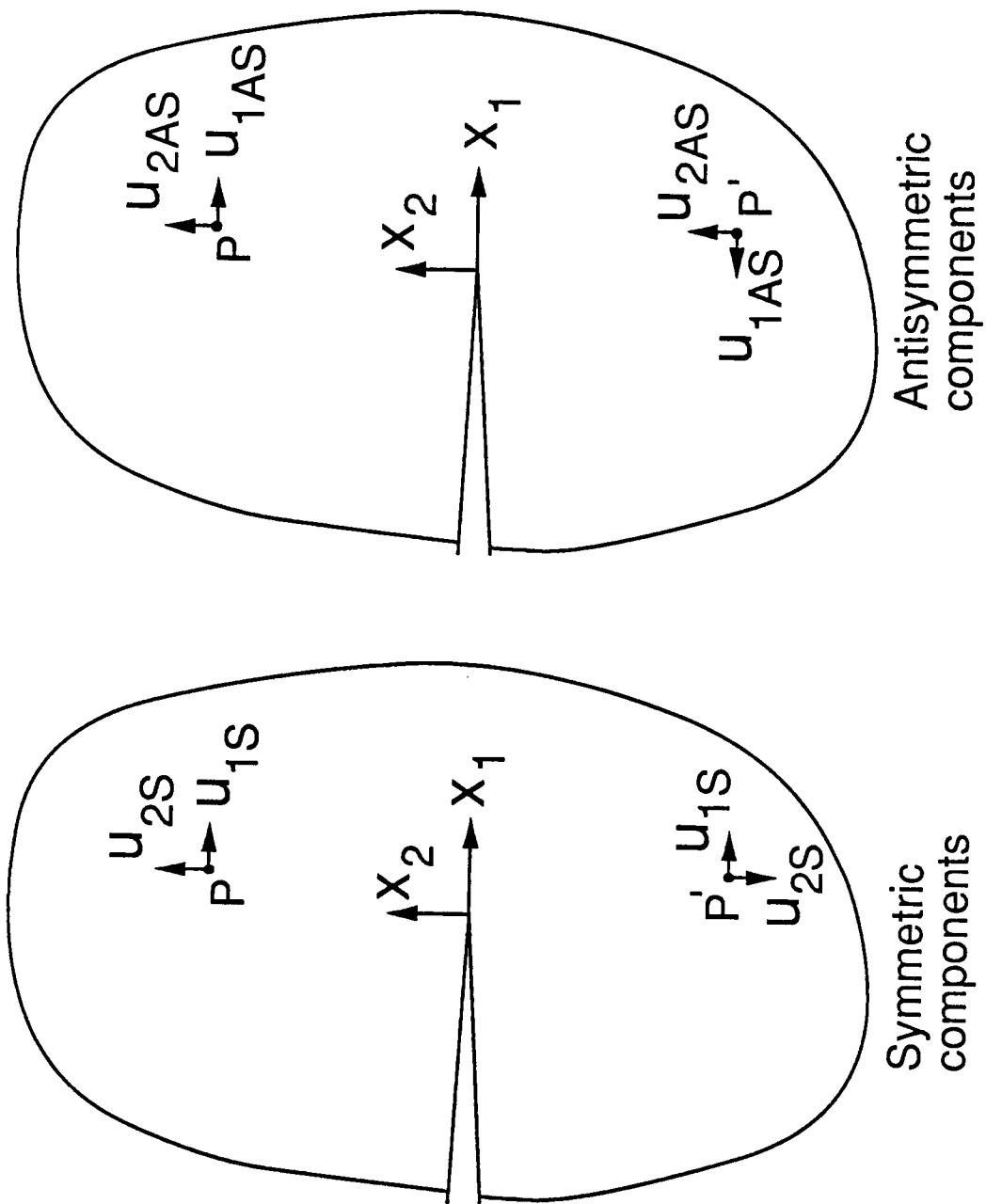


Figure 2 - Symmetric and antisymmetric displacement components.

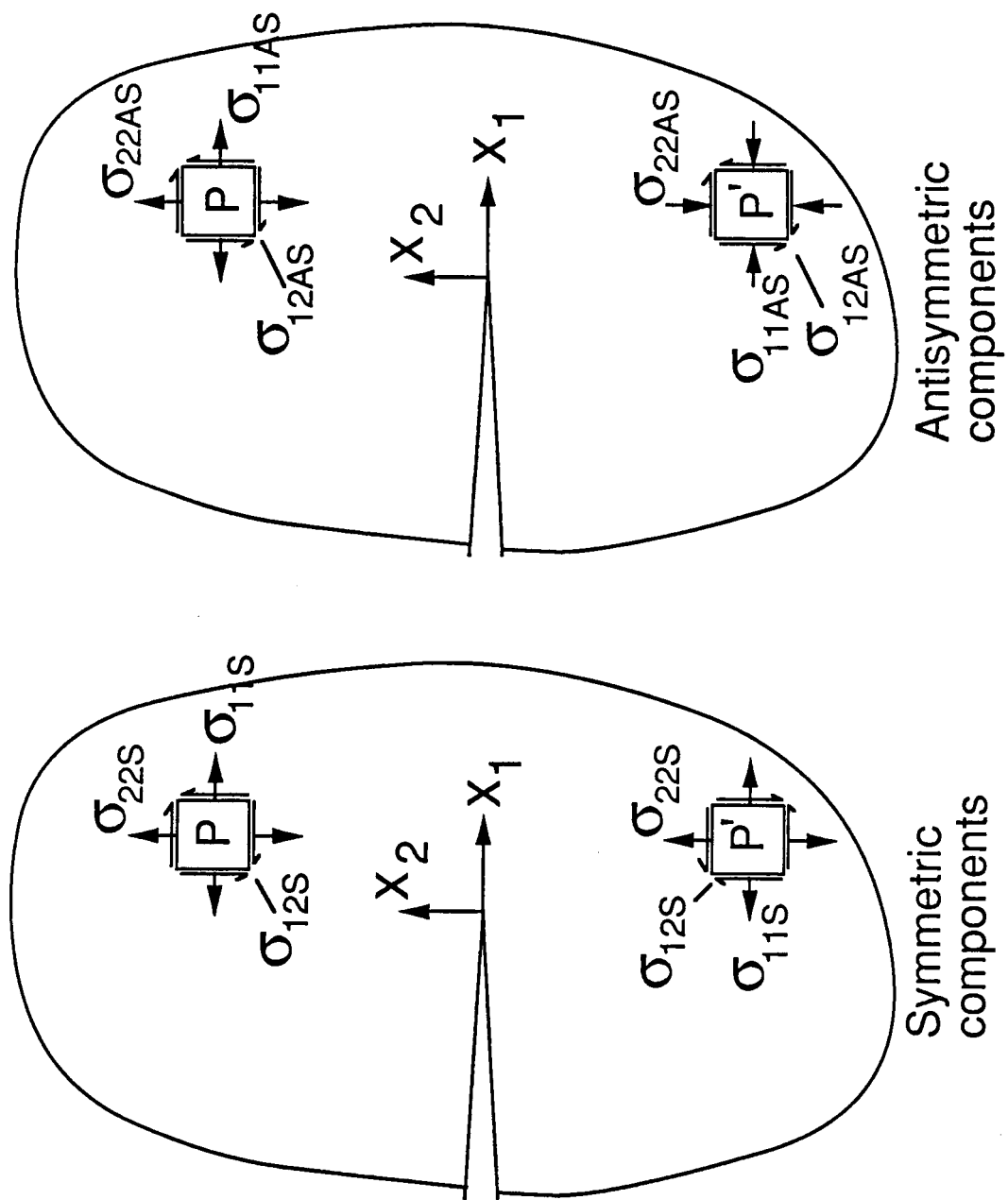
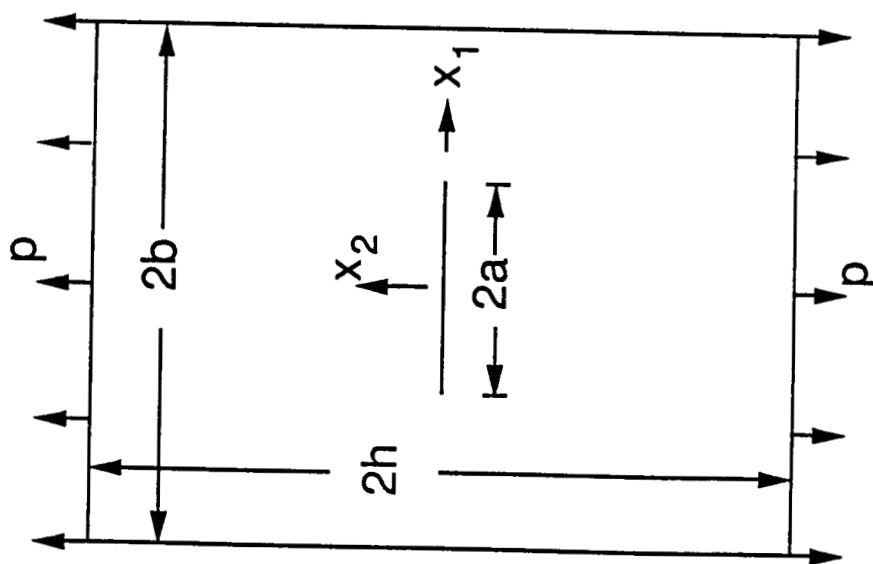
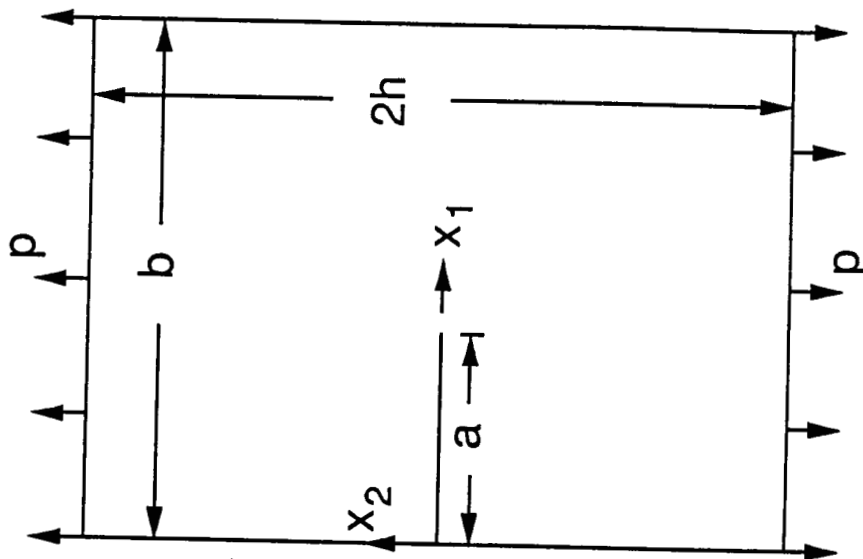


Figure 3 - Symmetric and antisymmetric stress components.

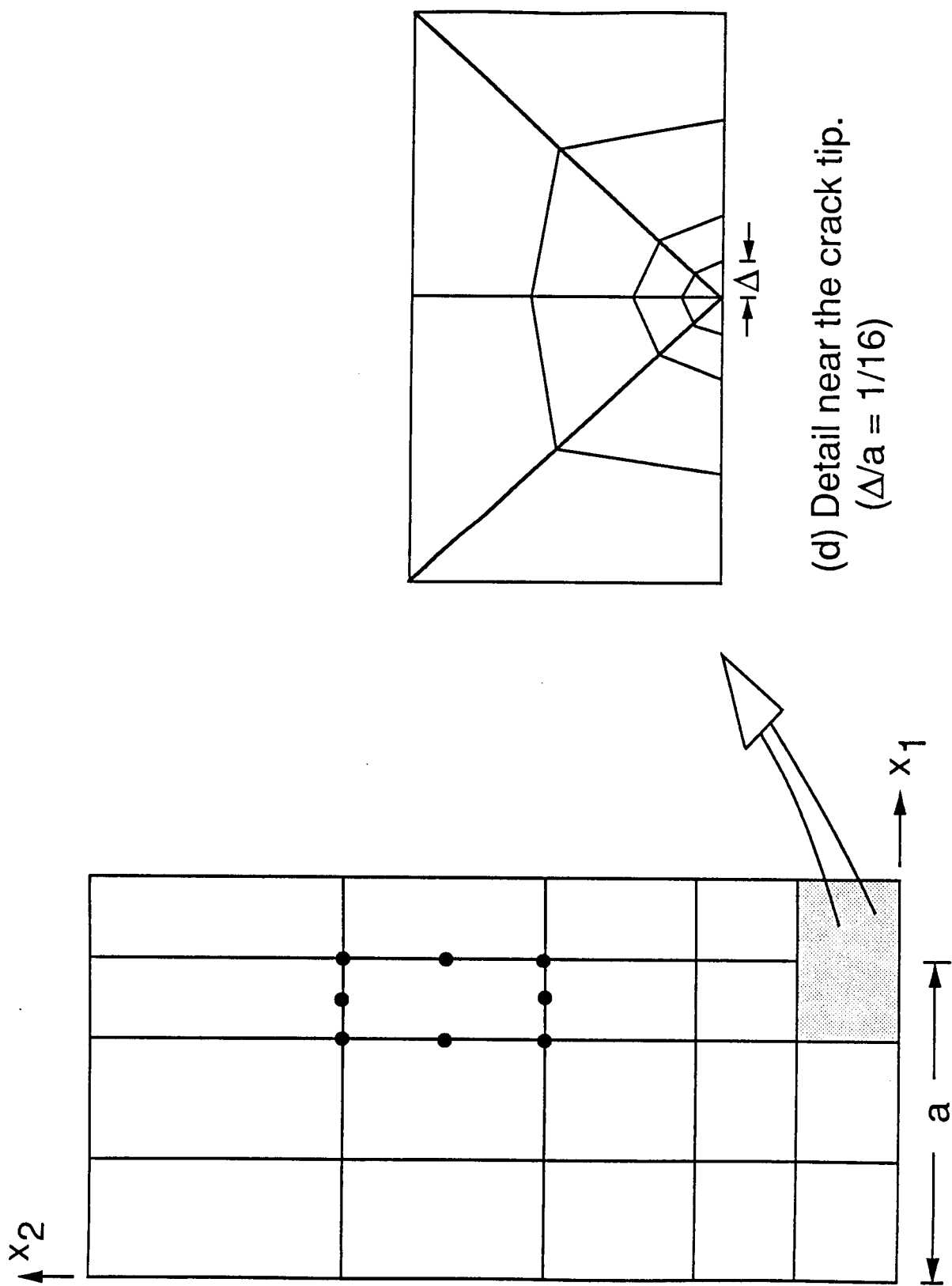


(a) CCT Specimen  
(  $h/b = 2.$ ;  $a/b = 0.8$  )



(b) SECT Specimen  
(  $h/b = 1.$ ;  $a/b = 0.8$  )

Figure 4 - Mode I problems and the finite element idealization.



(c) Finite element model.

Figure 4 - Concluded.

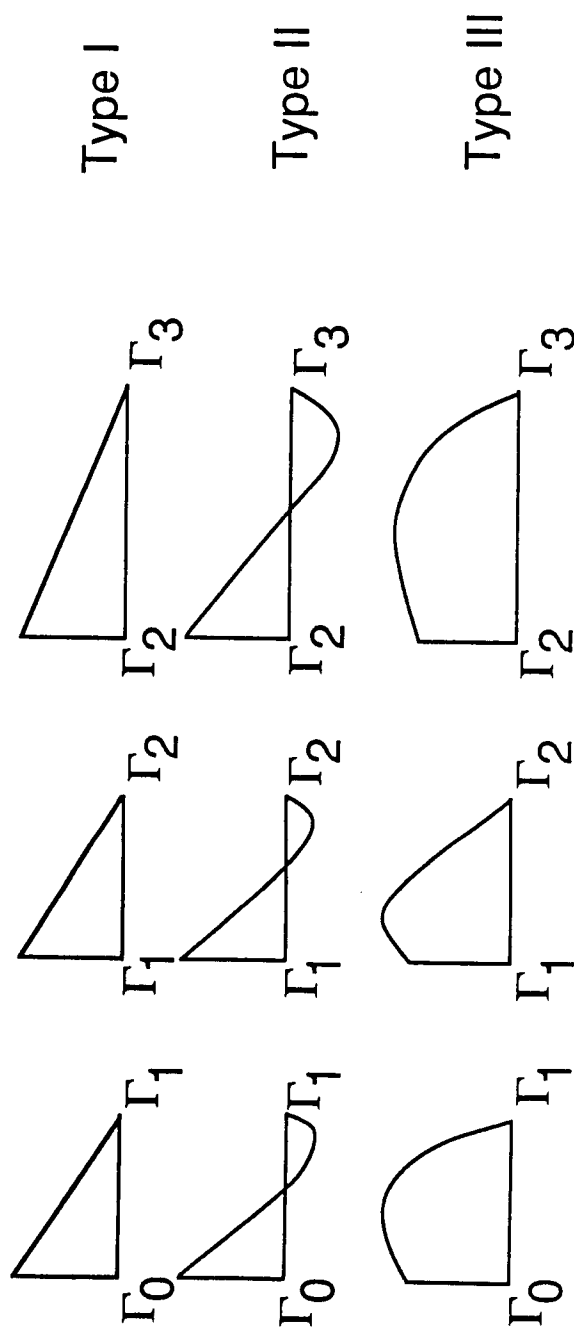
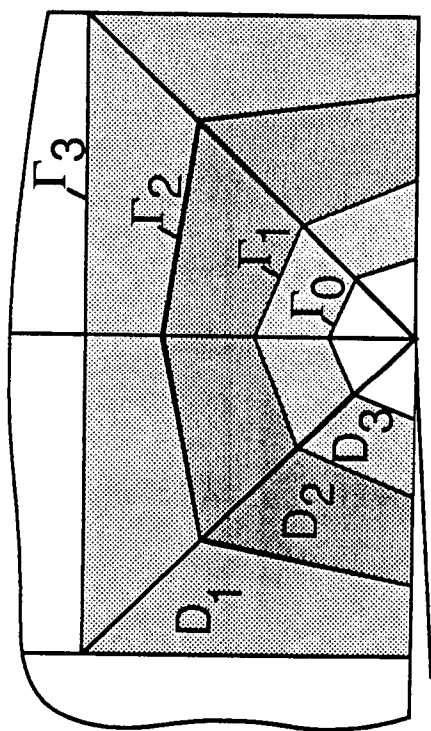
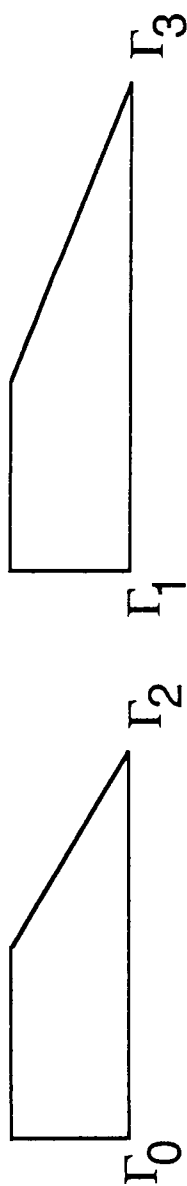
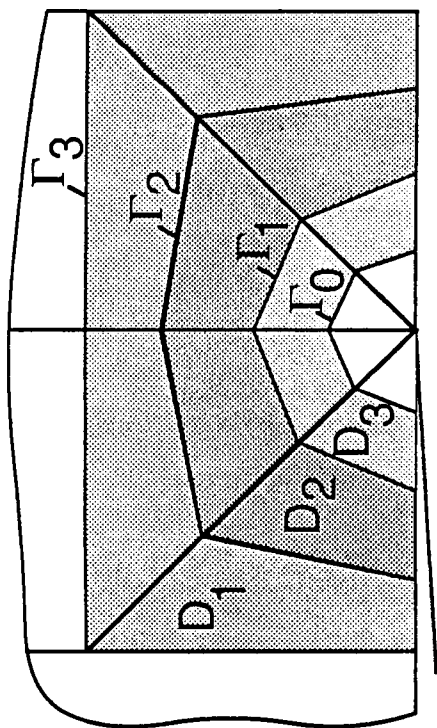
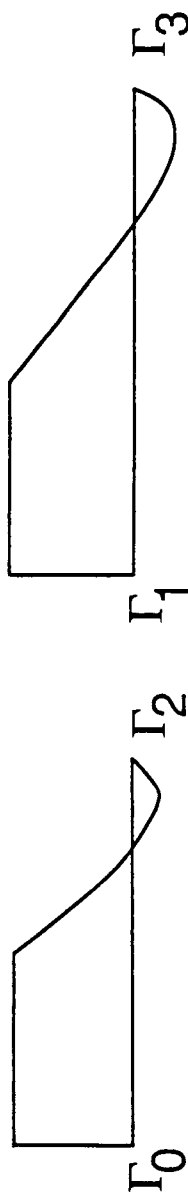


Figure 5 - Various domains and S-functions used in mode I problems.



Type IV



Type V

Figure 5 - Concluded.

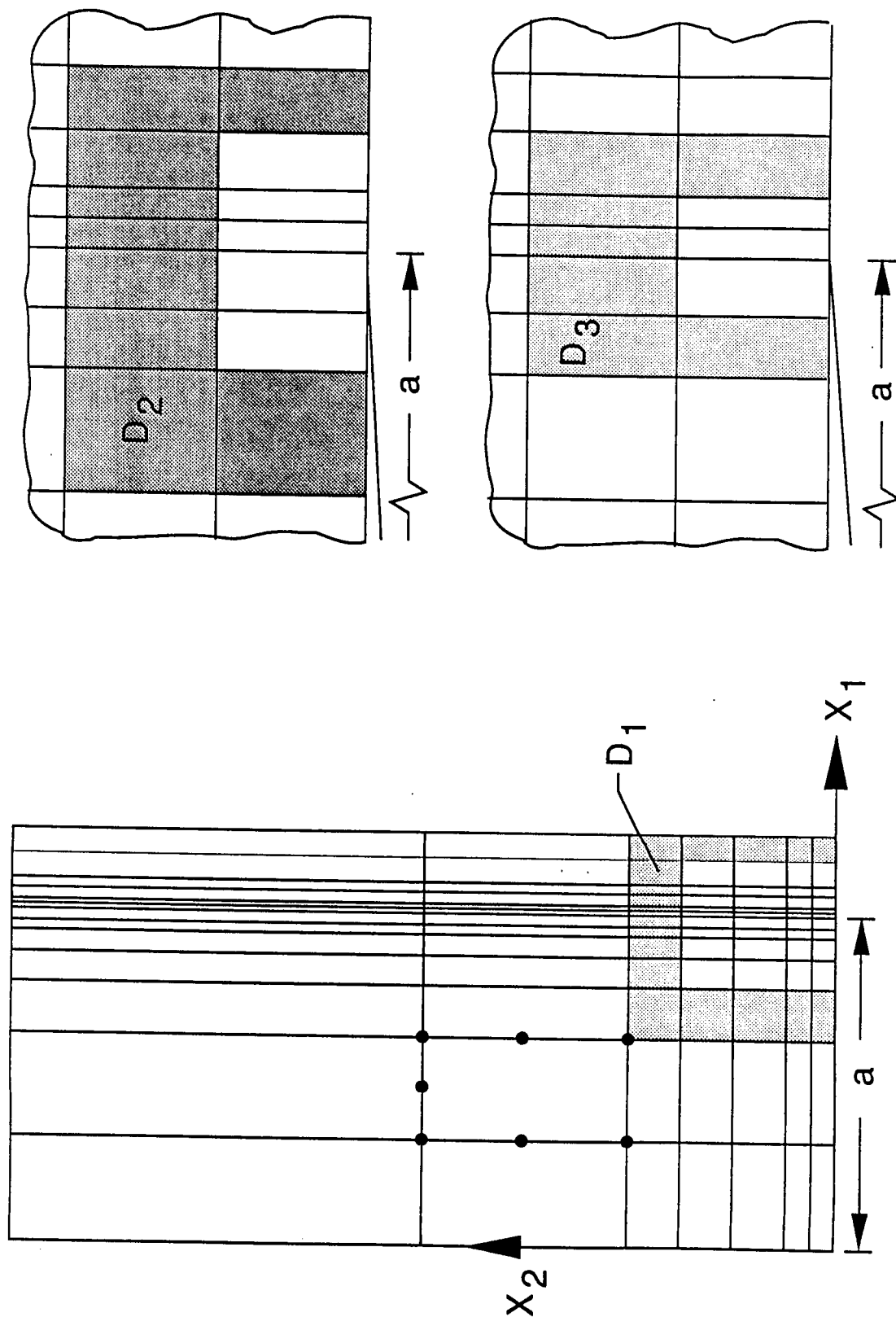
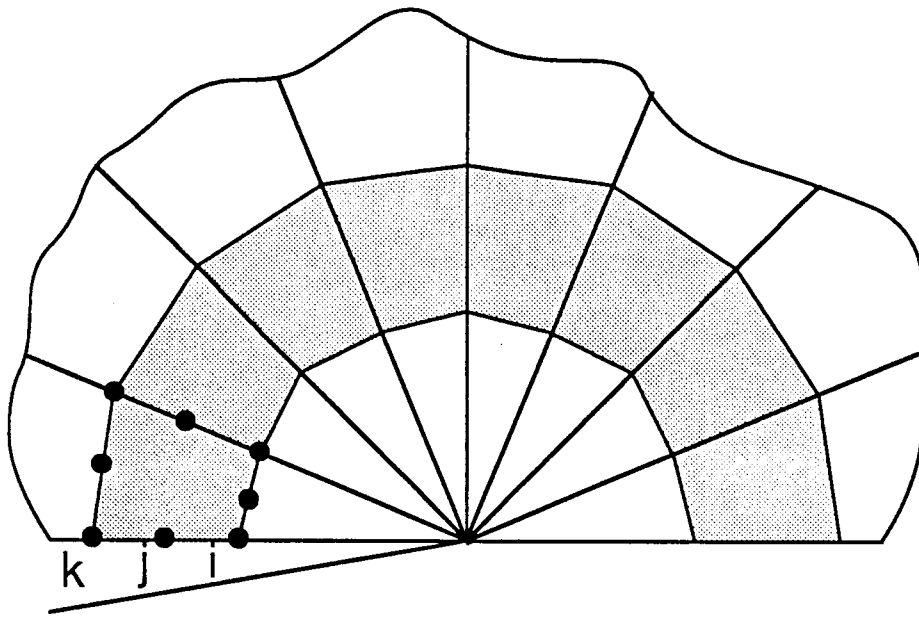
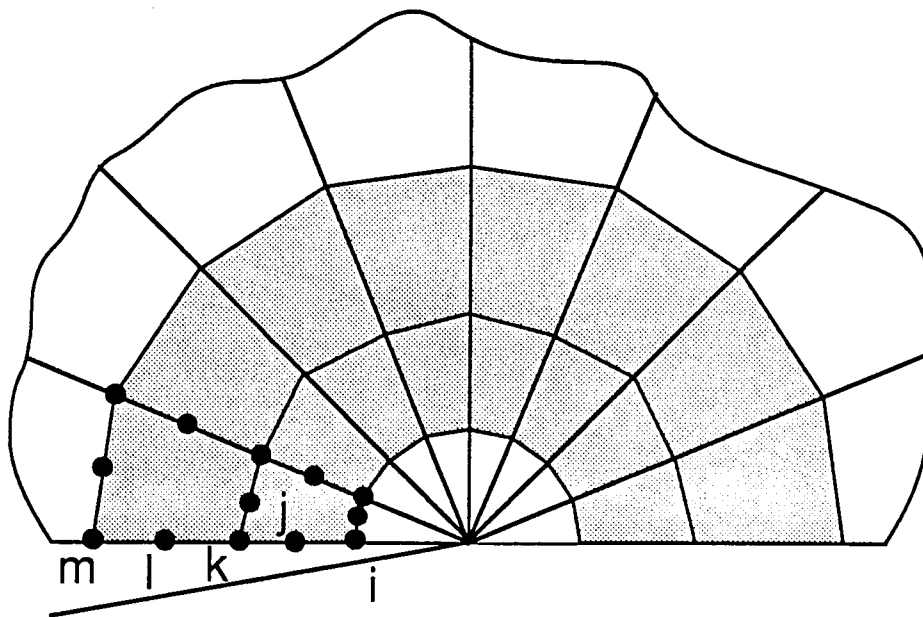


Figure 6 - Finite element model with non-singular elements and domains used in the EDI algorithm.

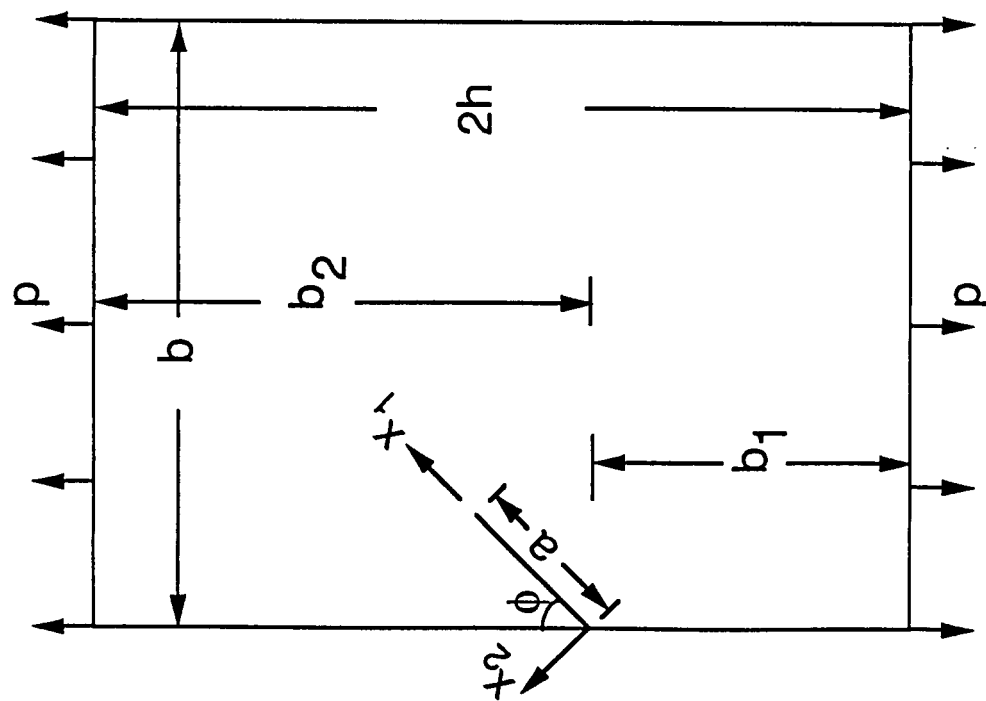


(a) Domain with one layer of elements.

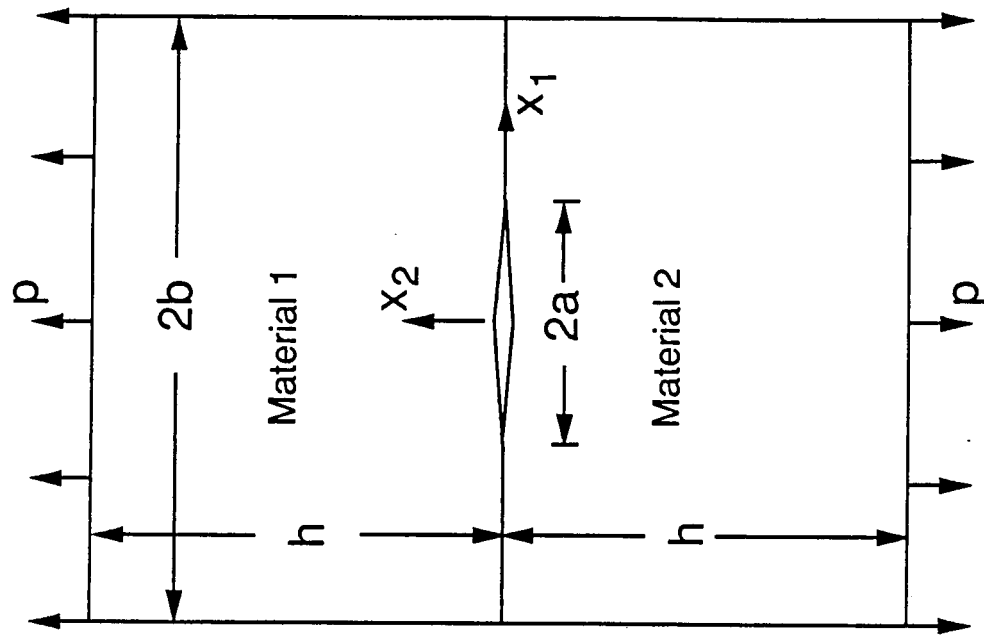


(b) Domain with two layers of elements.

Figure 7 - Nodes used in calculating the line-integrals for crack face pressure loading.

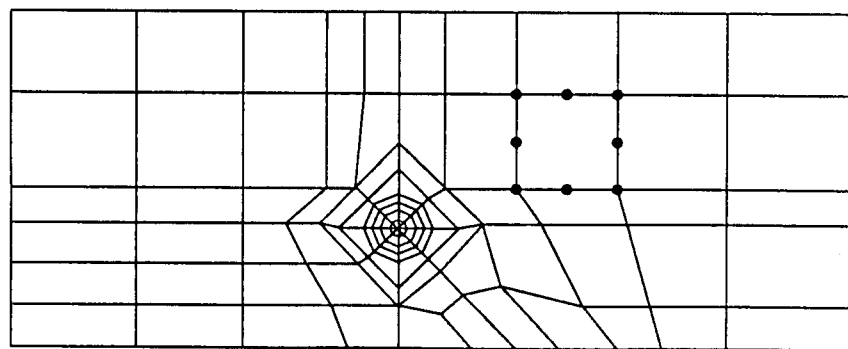


(a) Angle crack in a finite plate.  
 $(a/b = 0.5 ; b_1 = b ; b_2 = 1.5b ;$   
 $\phi = 45^\circ)$

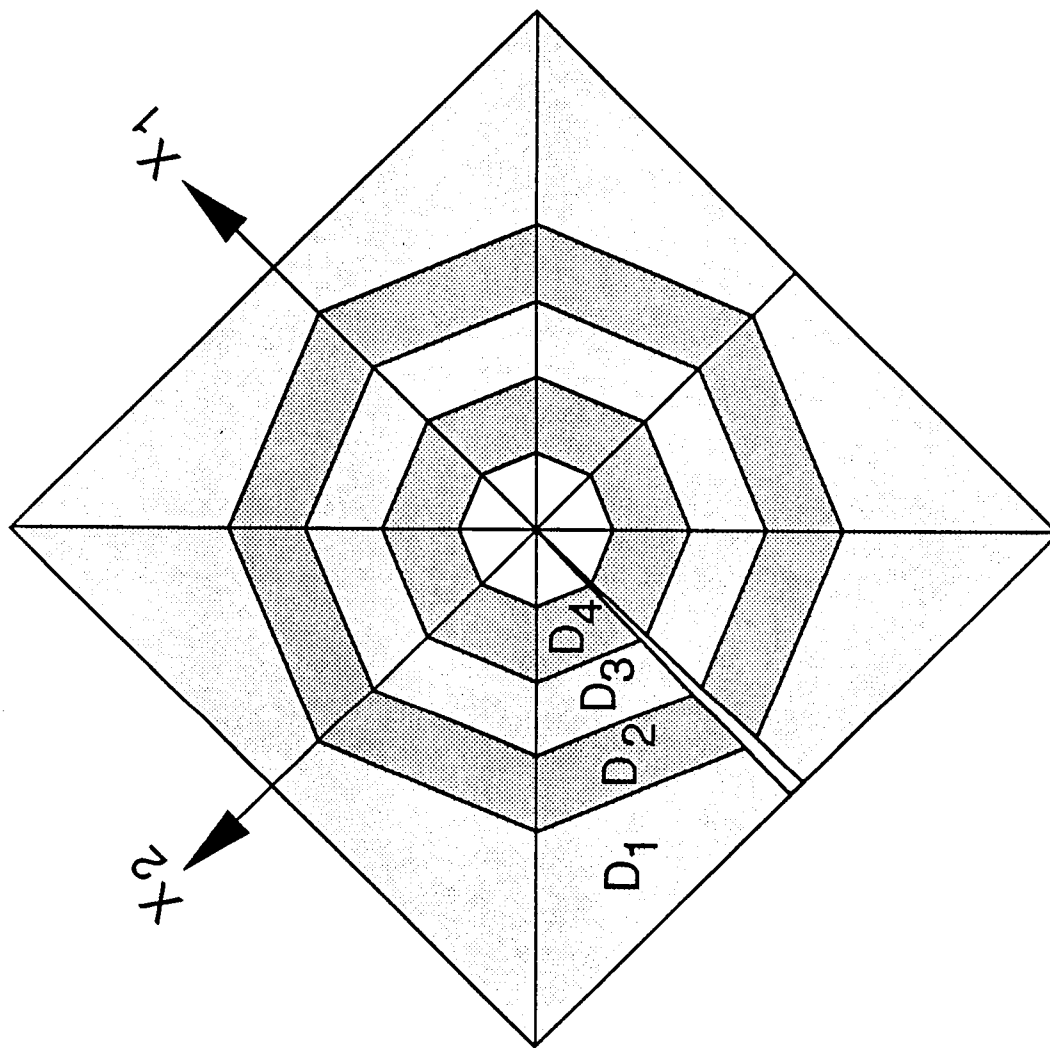


(b) Bimaterial plate with a central crack.  $(h/b = 1.5 ; a/b = 0.1)$

Figure 8 - Mixed mode problems.

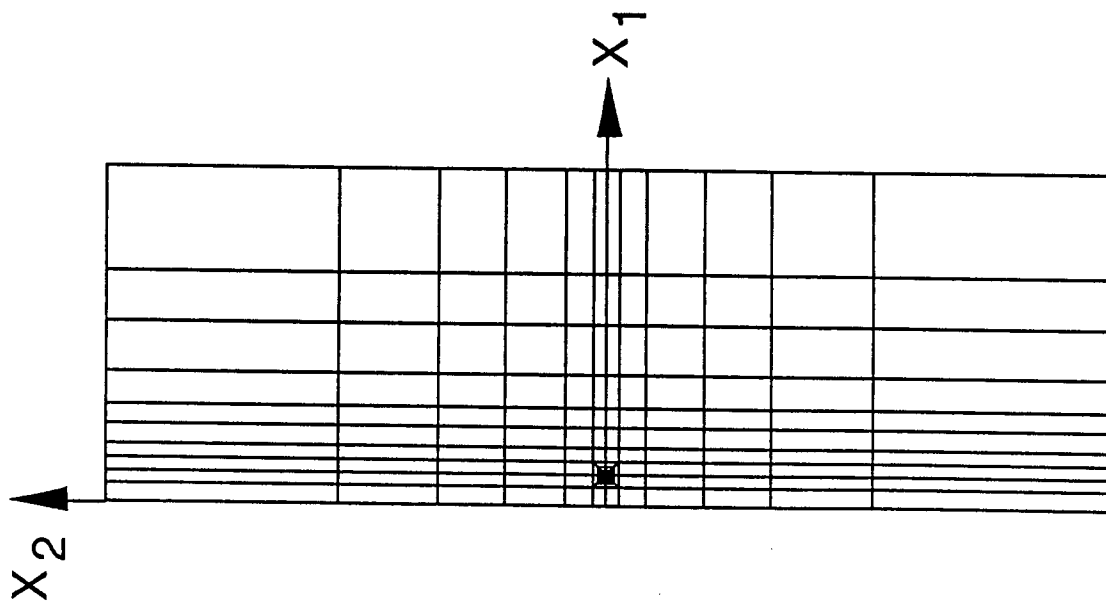


(a) Finite element model with 101 parabolic elements

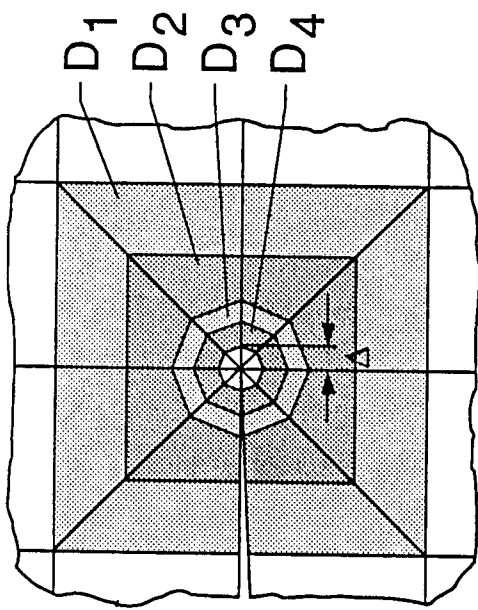


(b) Detail near the crack tip and domains used

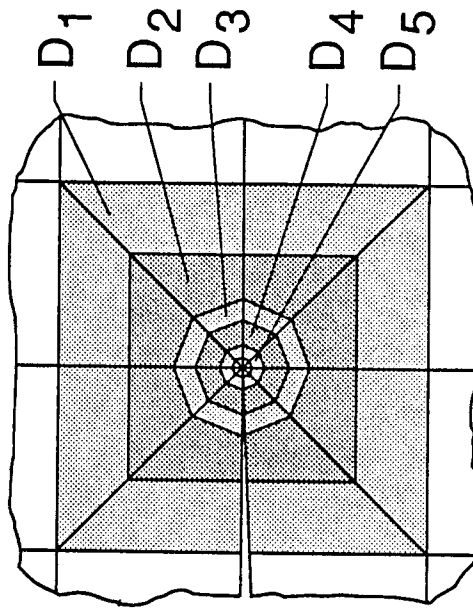
Figure 9 - Finite element model and domain used for the angle crack problem



(a) Finite element model



(b) Detail of modeling near the the crack tip  
for  $\Delta/a = 0.05$



(c) Detail of modeling near the the crack tip  
for  $\Delta/a = 0.025$

Figure 10 - Finite element idealizations and domains used for the bimaterial plate problem.

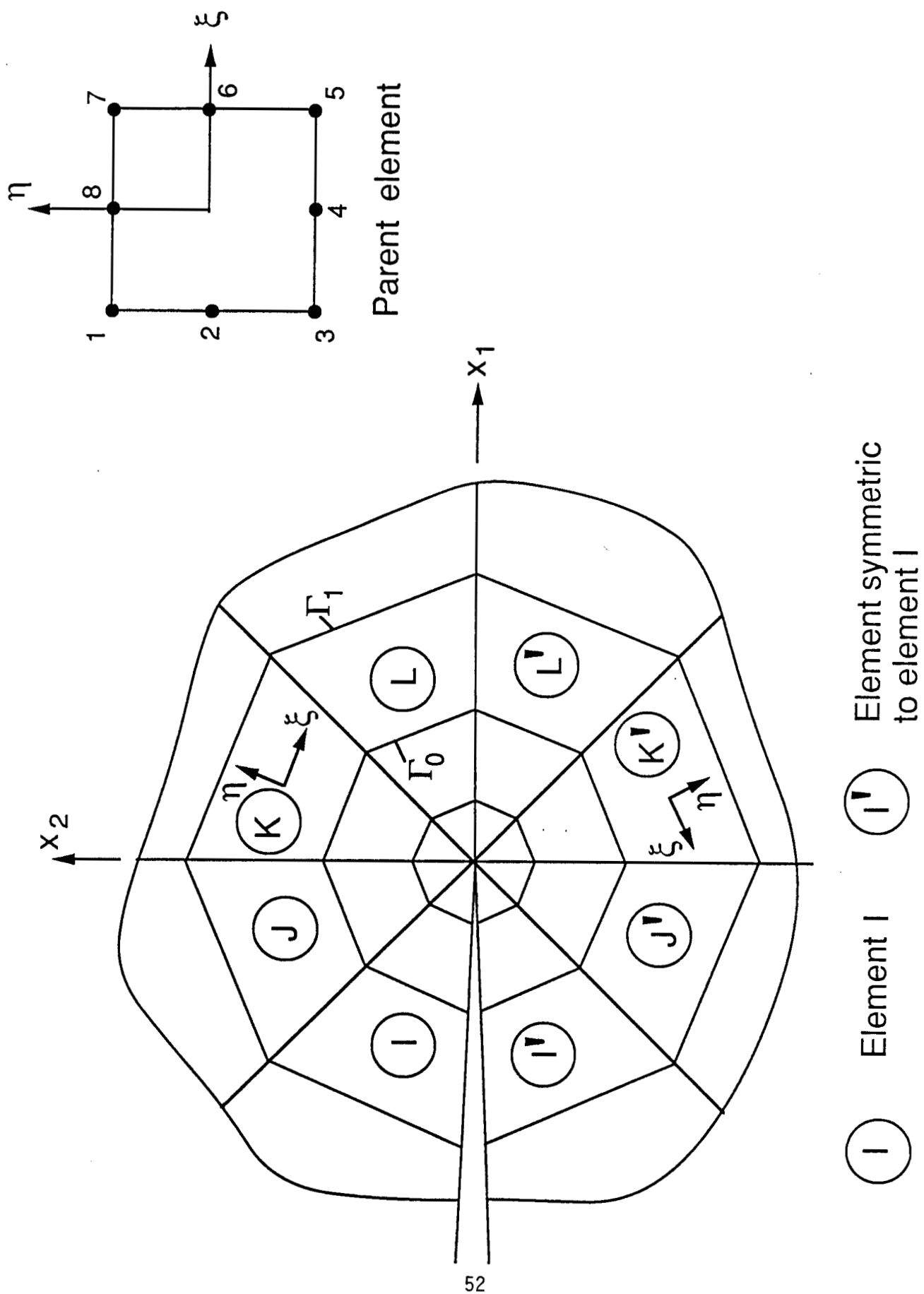


Figure A1 - Typical finite element model.

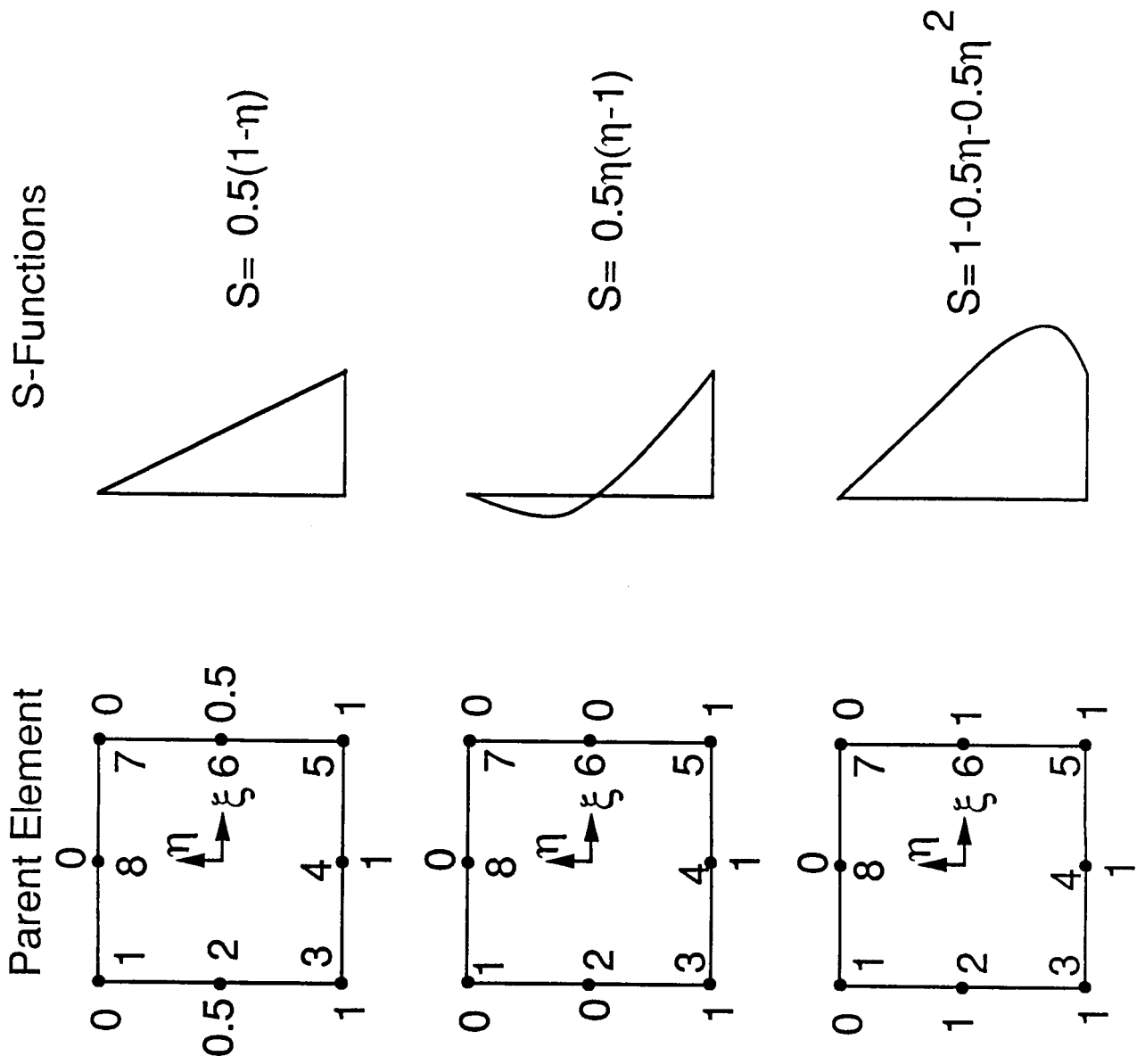


Figure A2 - Various S-functions.

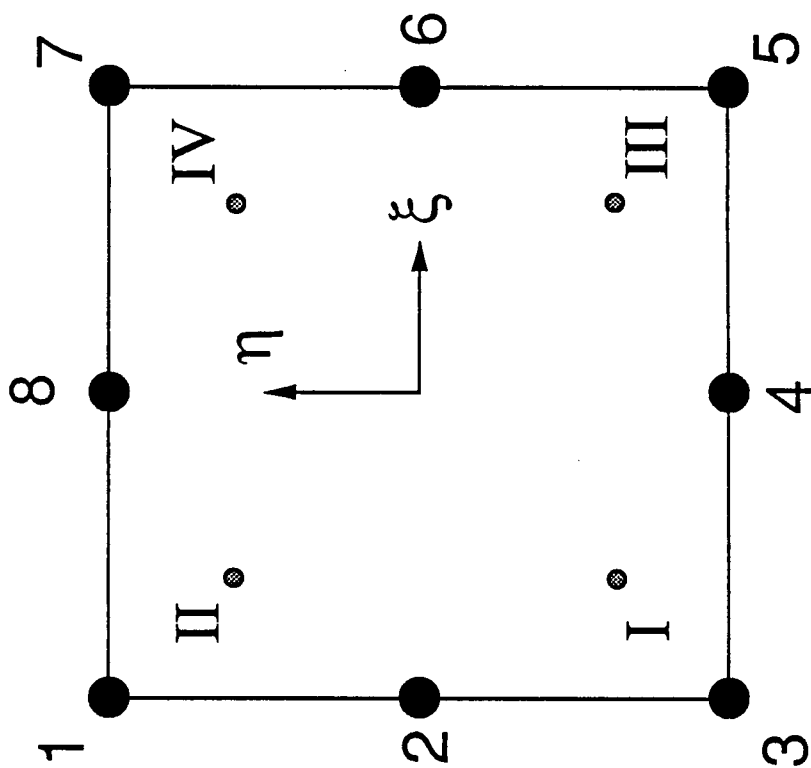


Figure A3 - 2x2 Gaussian quadrature points in the parabolic element.



## Report Documentation Page

1. Report No. <b>NASA CR-181813</b>	2. Government Accession No.	3. Recipient's Catalog No.	
4. Title and Subtitle <b>Implementation of Equivalent Domain Integral Method in the Two-Dimensional Analysis of Mixed Mode Problems</b>		5. Report Date <b>April 1989</b>	
		6. Performing Organization Code	
7. Author(s) <b>I. S. Raju and K. N. Shivakumar</b>		8. Performing Organization Report No.	
		10. Work Unit No. <b>505-63-01-05</b>	
9. Performing Organization Name and Address <b>Analytical Services and Materials, Inc. 107 Research Drive Hampton, VA 23666</b>		11. Contract or Grant No. <b>NAS1-18599</b>	
		13. Type of Report and Period Covered <b>Contractor Report</b>	
12. Sponsoring Agency Name and Address <b>National Aeronautics and Space Administration Langley Research Center Hampton, VA 23665-5225</b>		14. Sponsoring Agency Code	
15. Supplementary Notes  <b>Langley Technical Monitor: C. A. Bigelow</b>			
16. Abstract <p>An equivalent domain integral (EDI) method for calculating J-integrals for two-dimensional cracked elastic bodies is presented. The details of the method and its implementation are presented for isoparametric elements. The total and product integrals consist of the sum of an area of domain integral and line integrals on the crack faces. The line integrals vanish only when the crack faces are traction free and the loading is either pure mode I or pure mode II or a combination of both with only the square-root singular term in the stress field. The EDI method gave accurate values of the J-integrals for two mode I and two mixed mode problems. Numerical studies showed that domains consisting of one layer of elements are sufficient to obtain accurate J-integral values. Two procedures for separating the individual modes from the domain integrals are presented. The procedure that uses the symmetric and antisymmetric components of the stress and displacement fields to calculate the individual modes gave accurate values of the integrals for all problems analyzed. The EDI method when applied to a problem of an interface crack in two different materials showed that the mode I and mode II components are domain dependent while the total integral is not. This behavior is caused by the presence of the oscillatory part of the singularity in bimaterial crack problems. The EDI method, thus, shows behavior similar to the virtual crack closure method for bimaterial problems.</p>			
17. Key Words (Suggested by Author(s)) <b>Two-dimensional analysis Crack Equivalent domain integral J-integral Mixed mode fracture</b>		18. Distribution Statement  <b>Unclassified - Unlimited Subject Category - 39</b>	
19. Security Classif. (of this report) <b>Unclassified</b>	20. Security Classif. (of this page) <b>Unclassified</b>	21. No. of pages <b>55</b>	22. Price <b>A04</b>